

Gallé, Johannes; Katzenberger, Anja

Article — Published Version

Indian Agriculture Under Climate Change: The Competing Effect of Temperature and Rainfall Anomalies

Economics of Disasters and Climate Change

Suggested Citation: Gallé, Johannes; Katzenberger, Anja (2024) : Indian Agriculture Under Climate Change: The Competing Effect of Temperature and Rainfall Anomalies, Economics of Disasters and Climate Change, ISSN 2511-1299, Springer International Publishing, Cham, Vol. 9, Iss. 1, pp. 53-105, <https://doi.org/10.1007/s41885-024-00154-4>

This Version is available at:

<https://hdl.handle.net/10419/319154>

Standard-Nutzungsbedingungen:

Die Dokumente auf EconStor dürfen zu eigenen wissenschaftlichen Zwecken und zum Privatgebrauch gespeichert und kopiert werden.

Sie dürfen die Dokumente nicht für öffentliche oder kommerzielle Zwecke vervielfältigen, öffentlich ausstellen, öffentlich zugänglich machen, vertreiben oder anderweitig nutzen.

Sofern die Verfasser die Dokumente unter Open-Content-Lizenzen (insbesondere CC-Lizenzen) zur Verfügung gestellt haben sollten, gelten abweichend von diesen Nutzungsbedingungen die in der dort genannten Lizenz gewährten Nutzungsrechte.

Terms of use:

Documents in EconStor may be saved and copied for your personal and scholarly purposes.

You are not to copy documents for public or commercial purposes, to exhibit the documents publicly, to make them publicly available on the internet, or to distribute or otherwise use the documents in public.

If the documents have been made available under an Open Content Licence (especially Creative Commons Licences), you may exercise further usage rights as specified in the indicated licence.



<http://creativecommons.org/licenses/by/4.0/>



Indian Agriculture Under Climate Change: The Competing Effect of Temperature and Rainfall Anomalies

Johannes Gallé¹ · Anja Katzenberger²

Received: 11 March 2024 / Accepted: 12 June 2024 / Published online: 15 July 2024
© The Author(s) 2024

Abstract

The latest generation of global climate models robustly projects that monsoon rainfall anomalies in India will significantly increase in the 21st century due to global warming. This raises the question of the impact of these changes on the agricultural yield. Based on annual district data for the years 1966–2014, we estimate the relationship between weather indices (amount of seasonal rainfall, number of wet days, average temperature) and the most widely grown kharif crops, including rice, in a flexible non-parametric way. We use the empirical relationship in order to predict district-specific crop yield based on the climate projections of eight evaluated state-of-the-art climate models under two global warming scenarios for the years 2021–2100. We find that the loss in rice yield by the end of the 21st century lies on average between 3 - 22% depending on the underlying emission scenario. For the sustainable scenario impacts range from an increase of 3.2% to a decrease of 12.1% for individual districts. In the worst-case scenario, all districts are negatively affected, with a predicted decrease in rice yield ranging from 34% to a decrease of 11.5% in the long run. Potential gains due to increasing rainfall are more than offset by the negative impacts of increasing temperature. Adaptation efforts in the worst-case global warming scenario would need to cut the negative impacts of temperature by 50% in order to reach the outcome of the sustainable scenario.

Keywords Climate change · Monsoon · Agriculture · India

JEL Classification Q10 · Q54 · O53

Introduction

India is the second largest rice growing nation accounting for 24% of the world rice production in 2020 (FAO Faostat, 2022). Regarding export, India is the third largest exporter contributing 13% to global rice exports in 2020 (FAO Faostat, 2022). Besides this role on the global market, the stability of rice production has also an important impact on food security within the country since rice is the principal food crop in India with an overall production of 178

Both authors shared first-authorship.

✉ Johannes Gallé
Galle@mcc-berlin.net

¹ Mercator Research Institute on Global Commons and Climate Change, Berlin, Germany

² Potsdam Institute for Climate Impact Research & University of Potsdam, Potsdam, Germany

mio. tonnes in 2020. Further, more than 40% of the Indian labour force are employed in the primary sector (World Bank, 2022). The income of people employed in the primary sector is highly dependent on the annual weather realizations such as the Indian summer monsoon, which accounts for 80% of annual rainfall in India (Kumar, 2004, 2010). Thus, changes of the characteristics of the summer monsoon and the resulting income effects are highly relevant for the socioeconomic well-being of people in India (Jayachandran, 2006; Colmer, 2021; Allen and Atkin, 2022; Carleton, 2017; Rosenzweig and Binswanger, 1992; Taraz, Taraz, Chuang, 2019; Palagi, 2022).

As a result of global warming, it is expected and observed that the characteristics of Indian's climate, particularly the Indian summer monsoon, are undergoing a substantial change: Depending on the underlying emission scenario the surface air temperature in India is projected to increase by 1.3–4.4 °C by the end of the 21st century compared to a preindustrial reference period (Krishnan 2020). The temperature increase is accompanied by a projected increase in the amount of seasonal monsoon rainfall (Chaturvedi 2012; Menon et al. 2013; Ha 2020; authorname 2021) with an estimated increase ranging from +9.7% to 24.3% (authorname 2021) and an increase in the year-to-year variability (Menon et al. 2013; authorname 2021). It is projected that the number of very wet monsoon seasons increases by a factor of 5–8 (Katzenberger et al. 2022). Also on the subseasonal scale, the number of daily precipitation extremes is projected to increase (Krishnan 2020). This increase in climate variability on different scales will change the growing conditions for agricultural crops and therefore have an impact on the socio-economic livelihoods within India and given their role on the global market also beyond.

We focus on the question of how this projected increase in rainfall and temperature during the 21st century translates into agricultural production of Indian districts. Besides, we aim to assess the amount of adaptation that would be required to counteract negative impacts of global warming. To answer the research questions, we proceed as follows. First, we combine district data on agricultural outcomes for the years 1966–2014 with observed rainfall and temperature data during the same years to estimate the relation between agricultural yield and climate conditions in a flexible and non-parametric way. Second, we use the obtained coefficients in order to predict the future agricultural output for 2021–2100 on the basis of precipitation and temperature projections extracted from an evaluated set of 8 global climate models of the Coupled Model Intercomparison Project phase 6 (CMIP6). This comprehensive multi-ensemble approach complements previous research that provided first quantitative insights based on 'illustrative simulations'. In order to simulate different emission scenarios, we analyse the data of different Shared Socioeconomic pathways (SSPs).

We find opposing effects for rainfall and temperature on rice yield: On the one hand, there is a positive effect of the seasonal rainfall and the number of wet days during the monsoon season from June–September (JJAS). On the other hand, there is a strong negative impact of temperature during October and November (ON) on rice yield shortly before the crops are harvested. When applying the estimated coefficients to the projected future climate for the years 2021–2100, we find that agricultural yield is predicted to significantly decrease in the future unless adaptation measurements are implemented. This trend is most clear under the worst case global warming scenario (SSP5–8.5). Under this scenario, rice yield decreases on average by 22% relative to the years of 1994–2014 in the long-term (2081–2100). For the sustainable SSP1–2.6 scenario, the predicted losses in rice yield are more moderate with an average decrease of 3.4% in the long-term. These predicted decreases in rice yield are primarily driven by the negative impact of the projected future increase in temperature in ON, which dominates the potential gains due to increasing rainfall and the number of wet days during the monsoon season. This relationship holds for all major crops that are grown

during the monsoon in India except for sugarcane, which is predicted to benefit from climate change. We further show that it is especially the northern and eastern regions in India that are associated with the largest relative decreases. Similar spatial patterns occur when evaluating on the basis of the total rice production during the reference period (1995–2014). Midnapur district in West Bengal is associated with the strongest decrease by the end of the century, amounting to 160,550 tons (SSP1-2.6) and 786,132 tons (SSP5-8.5) respectively with an average total production of 2,611,253 tons during the reference period. Finally our results can be used to illustrate how potential adaptation in terms of gradually muting the negative impact of temperature in ON would change the predicted changes in rice yield. Thereby we are able to calculate the adaptation gap, which we define as the amount of adaptation that is required required in a world of unsuccessful climate change mitigation (SSP5-8.5) to reach the outcome of the sustainable scenario (SSP1-2.6), which depicts a world of successful climate change mitigation. In the long-term, we show that in the worst case scenario, the negative impact of temperature in ON would need to be cut by 50% in order to reach the predicted outcome of the sustainable scenario (average decrease of 3.4%).

The findings complement previous research that has examined the relationship between monsoon characteristics and rice yields based on past periods (Webster 1998; Meher 2015; Auffhammer 2012; Fishman 2016; Revadekar and Preethi 2012; Preethi 2019; Prasanna 2014; Panda 2019). The methodical approaches range from field measurements under different growing conditions over process-based models up to panel-based regression approaches. Auffhammer (2012) use fixed effects regressions in order to determine the effect of monsoon characteristics (extreme rainfall and drought, total rainfall and minimum temperature) on rice yield in India and use Monte-Carlo simulations to quantify the role of past climate change on the changes in kharif rice yield at the state-level between 1966–2002. The authors conclude that climate change has evidently already negatively influenced rice production in India. From a climatological perspective, it is important to note that the study is based on data covering the period 1966–2002. During these years, there was a dominating rainfall-reducing effect of aerosols on the Indian monsoon leading e.g. to increased occurrences of droughts (Seth 2019). This effect opposes the monsoon rainfall increasing effect imposed by greenhouse gases that is expected to be the leading forcing throughout the 21st century.

Regarding future predictions of rice yield under the influence of climate change, that are particularly important for future agricultural management (Fishman 2016; Taraz Taraz), only a limited number of studies are available: Singh (2017) use three climate models in order to quantify the relationship between rice cultivation and four climate indices. The authors find that the climate suitability of rain-fed rice locations is projected to decline between 15 and 40% by 2050. Fishman (2016) provides an ‘illustrative simulation’ of climate change impacts based on a projected 10% increase in precipitation and a decrease of rainy days by 15 - single values that are extracted from previous climate model generations. By using only a single value, the study neglects potential changes in the temporal and spatial distribution of rainfall and temperature. Thus, the author concludes that their approach may give a general idea of the tendency of future rice yield, but can not replace a complete climate model ensemble. Soora (2013) use the InfoCrop-rice model and one general circulation model as well as one regional climate model in order to quantify the impacts of climate change on rice yield. The authors find that the suitability of irrigated rice yields may decrease by 10% until 2070–2099. While the distribution of climate indices has been included in this study, there remains a strong dependency of the results on the choice of the single model, which is why this approach cannot replace a full ensemble model study.

There are numerous studies focusing on changes in global rice yield under climate change: Muller (2014) use the Land-Potsdam-Jena managed Land (LPJmL) as a widely

used ecosystem-based model and the Decision Support System for Agrotechnology Transfer (DSSAT) in combination with two climate models to quantify the global losses in rice production to be between 15.7 and 18.2% by 2050. Another study using these two process based models as well as 5 other global crop models find that models including explicit nitrogen stress project more severe impacts on global rice yield (Rosenzweig 2014). Zhao (2017) combine different methodical approaches (ranging from global grid-based and local point-based models, statistical regressions to field-warming experiments) to quantify the effect of an increase in global mean temperature on global crop yield. The authors find that per degree of global warming, global rice yield reduces by 3.2%. Vogel (2019) find that 27% of the variance in global rice yield in 1967–2008 are attributable to climate extremes. Katja et al. (2017) show that water limitation is a major driver of the observed variations in most countries in their study.

Section “Data” introduces the different data sources as well as the descriptive statistics of our final sample. The following Section “[Estimating the Effect of Rainfall and Temperature on Rice Yield](#)” provides the empirical methodology for estimating the effect of weather variables on agricultural yield as well as the results of the estimation. Section “[Climate Change Projections](#)” covers the future changes in predicted agricultural yield under different global warming scenarios. The final Section “[Conclusion](#)” discusses these results in the context of existing literature and concludes.

Data

For answering our research question on how climate change impacts agricultural production in India, we combine various data sets. The type of data can be grouped into three categories: agricultural production data from administrative records, observational weather data from the Indian Meteorological Department (IMD) as well as climate projections from 8 different climate models from the CMIP6.

Agricultural Data

We obtain information on annual agricultural output for Indian districts for the years 1966–2014 from the District Level Database (DLD) for Indian agriculture provided by the International Crops Research Institute for the Semi-arid Tropics (ICRISAT).¹ The DLD contains annual information on total production, yield and the share of irrigated area for all major crops in India. Given the focus of the study on the monsoon (kharif) season, we extract information on 7 crops, that are mainly grown during the monsoon season in India. These crops are rice, sorghum, maize, pearl millet, cotton, groundnut and sugarcane. The districts are apportioned to the district boundaries of 1966. Thereby the administrative boundaries are kept constant over time, which facilitates the construction of a balanced panel of Indian districts for the years 1966–2014. Overall the DLD contains information on 313 districts as of 1966, which corresponds to 571 districts as of 2014. Thereby, we cover 95% of the Indian population (as of the census 2011) and around 88% of the total area of India. The DLD information on annual crop production is collected from various administrative records such as the Ministry of Agriculture and Farmers Welfare or the different State Directorates of Agriculture.

¹ The data is freely accessible under the following link: <http://data.icrisat.org/dld/>.

Rainfall and Temperature Data

We complement the agricultural data with daily gridded rainfall and temperature data from the IMD. The rainfall data (IMD4) is available for the years 1901–2021 at a spatial resolution of $0.25^\circ \times 0.25^\circ$ (latitude \times longitude) (Pai 2014). The minimum and maximum temperature data is available for the years 1951–2020 at a spatial resolution of $1^\circ \times 1^\circ$ (latitude \times longitude) (Srivastava 2009). In order to calculate an estimation of the mean daily temperature, we average the minimum and maximum temperature. We spatially merge both of the data sets with the Indian district level data.² In case of multiple grid points located within one district, we take the mean of all grid points that fall within the boundaries of a single district. Based on the temporal and spatial distribution of daily rainfall and temperature, we construct 6 different variables. The first set of three variables is constructed over the months of June to September, which is commonly associated with the monsoon season in India. We calculate the average daily rainfall (which only differs by the absolute rainfall during the monsoon season by the factor of 122, given that JJAS consists of 122 days) and average temperature for each district in India for the months of June–September. Following (Fishman 2016), we calculate the number of wet days, which are defined as days with at least 0.1 mm of precipitation. We construct the same three variables for the post-monsoon season, which consists of the months of October and November and covers the time after the monsoon until the crops are usually harvested (Auffhammer 2012). Hence, our final set of weather variables consists of the *average daily rainfall* (JJAS & ON), the *average daily temperature* (JJAS & ON), as well as the *number of wet days* (JJAS & ON).³

Climate Model Data

Lastly, we use an evaluated set of the general circulation models that participated in the CMIP6 that recently has become publicly available.⁴ CMIP6 is a collaborative framework that coordinates climate modelling efforts around the world. In the context of each CMIP generation, the model groups provide standardized output of general circulation models covering past and future climate periods. Usually, each model generation is the basis for one Assessment Report of the Intergovernmental Panel on Climate Change (IPCC) that are published approx. every 6 years. The resolution of the native model grids differ strongly; an overview is given in Table 3. The models have been regridded and undergone bias correction in the context of the Inter-Sectoral Impact Model Intercomparison Project (ISIMIP) (Lange 2019).⁵ In order to gain insights into possible changes in crop yield, we use different emission scenarios. The scenarios are based on different socioeconomic development narratives that were translated into quantitative projections in several steps for, e.g., future energy systems, land use and greenhouse gas emission by the use of Integrated Assessment Models and transformed into input tables for the climate models. These scenarios are called Shared Socioeconomic Pathways (SSPs) (Van Vuuren 2014; O'Neill 2017) and are combined with

² For this purpose, we further construct a shapefile of Indian districts as of 1966.

³ Motivated by projected intensification of the monsoon on a daily scale (Katzenberger et al. 2022), we further constructed indices aiming to capture extreme weather events such as the number of heavy rainfall days (e.g. daily precipitation > 100 mm). Given, that these indices are almost perfectly correlated with average daily rainfall, we exclude the number of heavy rainfall days from the analysis.

⁴ The datasets from CMIP6 simulations are freely available via the CMIP6 Search Interface: <https://esgf-node.llnl.gov/search/cmip6/>

⁵ More details can be found in the ISIMIP3a protocol: <https://protocol.isimip.org/>

the corresponding forcing level for the future, the so called Representing Concentration Pathways (RCPs). In order to simulate unabated climate change, we use the scenario SSP5-8.5 which is the combination of the socio-economic scenario pathway 5 (SSP5) and the Representing Concentration Pathway 8.5 (RCP8.5). The pathway SSP5 is characterized by a global aspiration for continuous economic development and a subsequent energy intensive lifestyle. The resulting high energy demand is met with fossil fuels. In combination with a lack of global concern for environmental matters, this pathway results in potentially high challenges to mitigation of climate change. Furthermore, we use the scenario SSP1-2.6 that is characterized by a sustainable development accompanied by a reduction of carbon energy sources leading to low challenges for mitigation and adaptation (Van Vuuren 2014; O'Neill 2017). We choose these two scenarios to quantify the range of potential yield outcomes from minimum to maximum change. For all 8 models we extract the same 6 climate indices.

In order to classify the models with the best performance regarding the climate indices of interest, we conduct a model evaluation based on the reference period 1966–2014.⁶ In this context, we compare the historical simulations of 21 climate models that took part in CMIP6, with the above mentioned observed rainfall and temperature data from the IMD. The selection criteria are based on the climate indices relevant for this study. See 7.1 for details on the evaluation and model selection. Based on the results of the evaluation, we select 8 models that we use in our study: ACCESS-ESM1-5, CANESM5, IITM-ESM, INM-CM5-0, IPSL-797 CM6A-LR, KACE-1-0-G, NESM3, UKESM1-0-LL. By choosing a set of models, we can reduce the effect of model-specific bias and therefore derive a improved more general projection of future climate anomalies.

Descriptive Statistics

Table 1 shows descriptive statistics of our final district sample. The average rice yield over the period 1966–2014 amounts to $1,450 \frac{\text{kg}}{\text{ha}}$, with 44% of the area used for rice production irrigated. As can be seen in Panel (A) average daily rainfall, number of wet days and average daily temperature strongly differ by season. With an average daily rainfall of $7.3 \frac{\text{mm}}{\text{day}}$, the amount of rainfall during the monsoon season (JJAS) clearly dominates the annual rainfall cycle. On average, Indian districts experience 70.4 wet days during June–September (which refers to almost 60% during one season). For the months of October and November the share of wet days drops on average to 16%. Further, average daily temperature drops from 28°C in JJAS to 23.5°C in ON. Panels (B) – (D) summarize the averaged climate projections of the selected climate models. Panel (B) highlights the descriptive statistics for the years 1995–2014, which serves as our reference period when predicting the agricultural impacts of climate change. Panel (C) summarizes the projections for the years 2021–2100 for the sustainable scenario SSP1-2.6 and Panel (D) for the worst case scenario SSP5-8.5. For both, JJAS and ON, an increase in average daily rainfall, temperature and the number of wet days is projected throughout the 21st century for the sustainable as well as for the worst case scenario: Average JJAS rainfall in 2021–2100 increases by 15% relative to 1995–2014 for the SSP1-2.6 scenario and by 25% for SSP5-8.5. Further details regarding the individual periods can be found in IPCC (2022) or authorname (2021). With an increase by 13% (SSP1-2.6) and 16% (SSP5-8.5), the increase in the number of wet days (JJAS) differs less between the two scenarios. The strongest relative difference between the two SSPs is observed in the

⁶ The standardized historical simulations are in general available for the period 1850–2015. But for single models, the year 2015 was not available, which is why we shortened the period for the evaluation process by one year in order to create comparability between the models.

Table 1 Descriptives statistics

	(1) <i>Mean</i>	(2) <i>SD</i>	(3) <i>Min</i>	(4) <i>Median</i>	(5) <i>Max</i>	(6) <i>N</i>	(7) <i>Source</i>
(A) 1966 - 2014							
-Rice yield (kg/ha)	1,450	927.7	0	1,297	6,547	15,176	ICRISAT
-Rice production (1000t)	217.7	315.0	0	93.97	3,153	15,176	ICRISAT
-Share irrigated area	0.441	0.399	0	0.336	1	15,176	ICRISAT
JJAS							
-Average daily rainfall (mm/day)	7.263	4.385	0.0676	6.561	36.82	15,239	IMD
-Wet days (>0.1mm)	70.38	21.31	4.333	71.13	120.5	15,239	IMD
-Average daily temperature (°C)	27.98	2.141	21.29	28.36	33.36	15,239	IMD
ON							
-Average daily rainfall (mm/day)	1.571	2.104	0	0.781	19.27	15,239	IMD
-Wet days (>0.1mm)	9.782	9.426	0	6.727	56	15,239	IMD
-Average daily temperature (°C)	23.52	2.520	12.26	24.00	28.98	15,239	IMD
(B) 1995 - 2014 (Climate Models)							
JJAS							
-Average daily rainfall (mm/day)	8.256	5.592	0.462	7.010	58.57	7,460	CMIP6
-Wet days (>0.1mm)	61.79	18.44	13.56	60.31	120.6	7,460	CMIP6
-Average daily temperature (°C)	27.60	3.938	6.167	28.55	33.26	7,460	CMIP6
ON							
-Average daily rainfall (mm/day)	1.953	2.137	0.0154	1.187	16.46	7,460	CMIP6
-Wet days (>0.1mm)	11.08	7.250	2.438	8.875	60.25	7,460	CMIP6
-Average daily temperature (°C)	23.43	4.782	-3.860	24.63	28.96	7,460	CMIP6
(C) 2021 - 2100 (Climate Models: SSP1-2.6)							
JJAS							
-Average daily rainfall (mm/day)	9.553	5.855	0.538	8.499	57.99	29,840	CMIP6
-Wet days (>0.1mm)	70.01	16.69	15.73	68.81	120.9	29,840	CMIP6
-Average daily temperature (°C)	28.61	3.873	7.152	29.51	34.75	29,840	CMIP6
ON							
-Average daily rainfall (mm/day)	2.240	2.326	0.0198	1.397	18.95	29,840	CMIP6
-Wet days (>0.1mm)	13.28	8.748	2.333	10.44	60.63	29,840	CMIP6

Table 1 continued

	(1) <i>Mean</i>	(2) <i>SD</i>	(3) <i>Min</i>	(4) <i>Median</i>	(5) <i>Max</i>	(6) <i>N</i>	(7) <i>Source</i>
-Average daily temperature (°C)	24.64	4.673	-2.720	25.86	30.19	29,840	CMIP6
(D) 2021 - 2100 (Climate Models: SSP5-8.5)							
JJAS							
-Average daily rainfall (mm/day)	10.32	6.195	0.827	9.133	65.58	29,840	CMIP6
-Wet days (>0.1mm)	71.77	15.54	18.27	71.25	120.9	29,840	CMIP6
-Average daily temperature (°C)	29.94	4.031	7.049	30.68	38.27	29,840	CMIP6
ON							
-Average daily rainfall (mm/day)	2.587	2.507	0.0251	1.790	22.84	29,840	CMIP6
-Wet days (>0.1mm)	14.72	8.865	2.750	12.06	60.25	29,840	CMIP6
-Average daily temperature (°C)	26.19	4.776	-2.966	27.24	33.67	29,840	CMIP6

Notes: Sample consists of a panel of 313 districts for the years 1966–2014. District boundaries are drawn as of 1966. Sources for agricultural output from ICRISAT. Temperature and rainfall data is obtained from IMD. In cases of missing observations for irrigated area, the information has been interpolated from the closest earlier year with information on irrigated share. Weather variables are calculated for the months June–September (JJAS), which refers to the monsoon season and for the months October–November (ON), which refers to the post monsoon season until the kharif crops are harvested. The climate model projection data is reported as the mean of 8 selected climate models (CMIP6)

respective projections of JJAS average daily temperature, where the 8% increase relative to 1995–2014 in the SSP5-8.5 scenario is twice as high as the increase in the SSP1-2.6 Scenario (4%). Similar tendencies can be observed for the post-monsoon season, where the relative difference between the SSPs is most pronounced for average daily temperature. The SSP5-8.5 scenario is associated with an increase of 12%, while the SSP1-2.6 scenario projects an increase by 5%.

Estimating the Effect of Rainfall and Temperature on Rice Yield

Empirical Approach

Our methodological approach is summarized in Fig. 8. The two main challenges in identifying a causal impact of weather realizations (e.g. precipitation and temperature) on agricultural output are the endogeneity of the explanatory weather variables as well as the a-priori unknown functional relationship between weather and agricultural output (Schlenker and Roberts 2009). By constructing a panel of Indian districts for the years 1966–2014, we rely on annual variation within districts for identifying the causal impact of our constructed weather variables on agricultural output. This variation can be plausibly seen as exogenous and is well established in the literature (Dell 2014; Chen et al. 2016; Hsiang 2016; Zhang et al. 2017; Auffhammer 2020). In order to put as less restrictions as possible on the functional

form for identifying the effect of weather on agricultural output, we follow an approach similar to Schlenker and Roberts (2009); Deschenes and Greenstone (2011) and Dell (2012). We group the weather variables into different bins based on their observed distribution for the years 1966–2014. This allows for maximum flexibility in estimating the effect of weather on our outcome of interest. The only functional assumption we impose is that the effects are constant within the same bin.

The main analysis relies on a model of the following form:

$$\begin{aligned}
 \ln(y_{it}) = & \underbrace{\sum_{a=1, a \neq \bar{a}}^{37} \beta_a \text{rainfall}_{a_{it}} + \sum_{b=5, b \neq \bar{b}}^{125} \beta_b \text{wetdays}_{b_{it}} + \sum_{c=22, c \neq \bar{c}}^{34} \beta_c \text{temp}_{c_{it}}}_{\text{Monsoon (JJAS)}} \\
 & + \underbrace{\sum_{d=0, d \neq \bar{d}}^{20} \beta_d \text{rainfall}_{d_{it}} + \sum_{e=0, e \neq \bar{e}}^{60} \beta_e \text{wetdays}_{e_{it}} + \sum_{f=13, f \neq \bar{f}}^{29} \beta_f \text{temp}_{f_{it}}}_{\text{Post Monsoon (ON)}} \\
 & + \beta_5 \text{irrigation}_{it} + \alpha_i + \gamma_t + \epsilon_{it},
 \end{aligned} \tag{1}$$

where y_{it} stands for the crop yield (e.g. rice; in $\frac{\text{kg}}{\text{ha}}$) in district i in year $t \in [1966, 2014]$. $\text{rainfall}_{a_{it}}$ refers to the average daily rainfall during JJAS, which we group into 37 bins of 1mm. Hence, $\text{rainfall}_{1_{it}}$ is equal to 1 if district i in year t obtained an average daily rainfall $\in (0\text{mm}, 1\text{mm}]$ and $\text{rainfall}_{2_{it}}$ equals 1 if average daily rainfall $\in (1\text{mm}, 2\text{mm}]$. $\text{rainfall}_{37_{it}}$ equals 1 if average daily rainfall $\in (36\text{mm}, 37\text{mm}]$ and thereby covers the upper end of the rainfall distribution in our estimation sample. We omit $\text{rainfall}_{8_{it}}$, which represents the mean of the distribution of average daily rainfall in our sample for JJAS. Hence, the coefficients β_a have to be interpreted relative to the mean average daily rainfall. $\text{wetdays}_{b_{it}}$ refers to the the binned number of wet days, which range from a minimum of 5 wet days up to 121 wet days during JJAS. Each bin exclusively contains 5 consecutive wet day counts. Accordingly, $\text{wetdays}_{5_{it}}$ equals 1 if the number of wet days during JJAS in district i in year $t \in (0, 5]$. Again we exclude the average value $\text{wetdays}_{75_{it}}$. We repeat the same procedure for $\text{temp}_{c_{it}}$, where we group average daily temperature during JJAS into 1°C bins ranging from 22°C to 34°C . We omit the mean bin $\text{temp}_{29_{it}}$. Analogously, we proceed with $\text{rainfall}_{d_{it}}$, $\text{wetdays}_{d_{it}}$ and $\text{temp}_{f_{it}}$, which are constructed over the months of October and November. In addition to the weather variables, we include the share of irrigated land irrigation_{it} . We further add district fixed effects α_i to control for time-invariant differences across districts as well as year fixed effects γ_t accounting for annual shocks that are common to all districts, which also accounts for general technological progress in terms of efficiency in agriculture. ϵ_{it} is the error term.

Estimation Results

Since rice is the principal food grain that is grown during the monsoon season in India, we choose rice yield as the dependant variable for illustrating our empirical results.⁷ Figure 1 plots the estimation results of Eq. 1 using the log of rice yield as the dependent variable. The estimated $\hat{\beta}$'s are given separately in Panels (a) - (f) for each of the main explanatory

⁷ Estimation results on other major kharif crops are reported in Figs. 9 - 14 in 7.1.

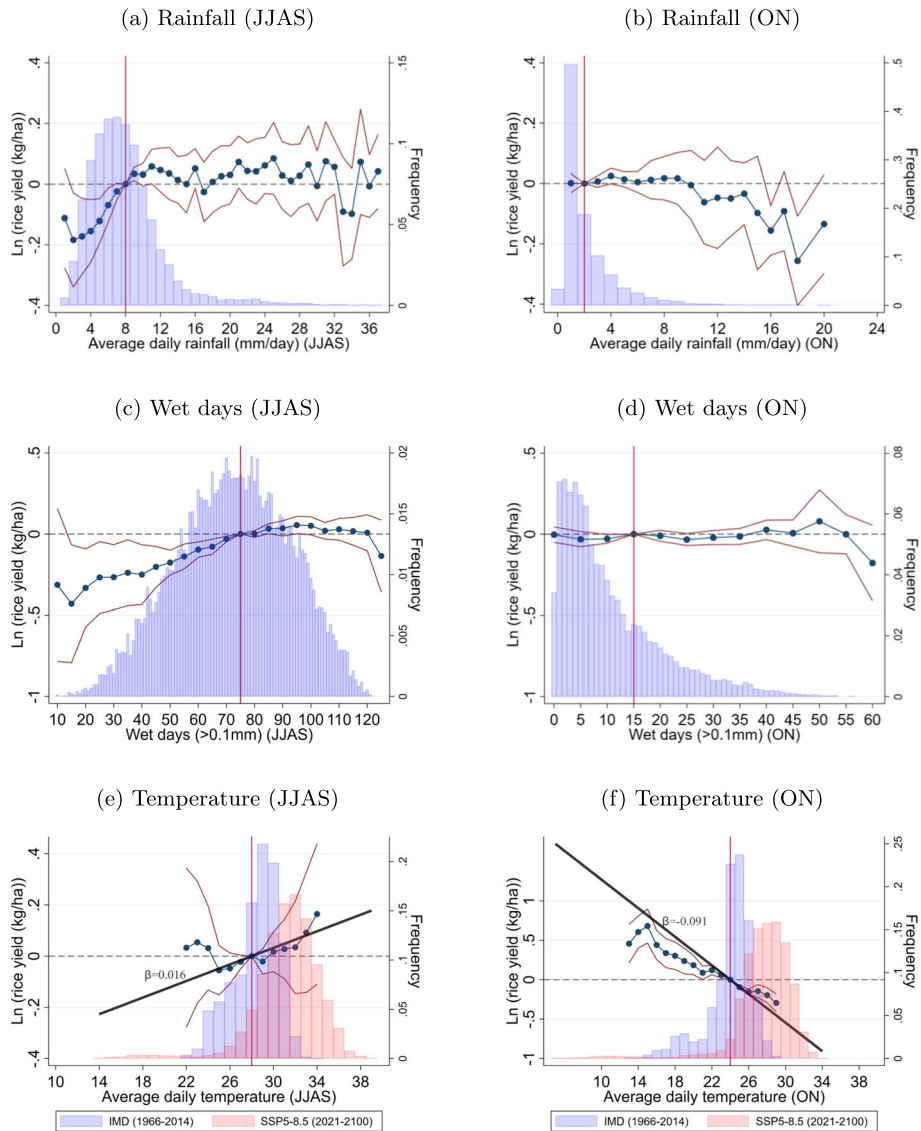


Fig. 1 Estimation results for rice. The plotted coefficients refer to the coefficients $\hat{\beta}$ as estimated according to Eq. 1. Red lines indicate the respective 95% confidence interval. The vertical red line refers to the omitted bin, which corresponds to the sample mean. Panel (a) depicts the results for average daily rainfall for the months of June, July, August and September (JJAS) on rice yield. Panel (b) - (f) depict the results for the remaining variables. Standard errors are clustered at the state level. The regression further includes district and year fixed effects, which are not reported. The blue colored bars display the binned distribution of the respective variables based on the the years 1966-2014. Red bars display the projected temperature distribution under SSP5-8.5. Data sources: ICRISAT, IMD, CMIP6

variables. Red lines indicate the respective 95%-confidence intervals and the blue colored bars in the background show the underlying distribution of the observed values (1966-2014) that is used for identification. Panel (a) shows the results for average daily rainfall in JJAS.

The impact of rainfall on rice yield is not symmetrically distributed around the mean. While a drop in average daily rainfall by 50% from the sample mean (from 8 mm/day to 4mm/day) reduces the rice yield on average by 12 percentage points (*pp*) ($= (e^{-0.137} - 1) \times 100$), an increase in rainfall by the same amount (from 8 mm/day to 12mm/day) increases the rice yield on average only by 5*pp*. Generally, additional rainfall beyond the mean has no significant impact on the rice yield (except for 9mm/day). The responsiveness of rice yield to rainfall in ON is very limited (Panel (b)). Yet, there is a downward sloping trend for rainfall extremes at the upper end of the rainfall distribution, i.e. excessive rainfall in the post monsoon season negatively impacts the rice yield. Average daily rainfall in ON of 18 mm/day decreases the rice yield on average by 18*pp* relative to districts with an average daily rainfall of 2mm/day. Note however, that these events are extremely rare and account only for 0.03% of the observations in our sample. As depicted by Panel (c), there is a positive impact of the number of wet days with a peak at 93 wet days. The impact of wet days (ON) is very limited with most coefficients being insignificant without showing any clear positive or negative pattern (Panel (d)). Lastly, Panel (e) and (f) depict the results for the average daily temperature in JJAS and ON respectively. While there is on average a slight positive but insignificant association between average daily temperature in JJAS and rice yield, there is a strong negative and significant association between average daily temperature during ON and rice yield. An increase in average daily temperature (ON) from 24°C by 5°C to 29°C decrease the rice yield on average by 28*pp*.

The main benefit of our estimation approach is to allow for a maximum degree of flexibility in delineating the impact of specific weather variables on crop yield. One shortcoming of this approach is that we can only identify effects of events that have been in the observable range of weather phenomena in the past. Using temperature in ON as an example, we can identify the impact of average daily temperature (ON) on rice yield within the range of 13°C to 29°C. Yet, with the estimates based on historical weather observations we cannot say anything about temperature exceeding 29°C. However, as shown by the red bars in Panel (e) and (f) of Fig. 1 a non-negligible share of projected temperature values (both in JJAS and ON) exceeds the range that has been observed in the past.⁸ Based on the observed functional form of the binned estimates, we assume a linear relationship between rice yield and temperature. We replace the temperature bins in Eq. 1 with a linear temperature term for both JJAS and ON. This allows us to extrapolate the impact of temperature increase that exceed past observations assuming a continuation of a linear relationship. The updated regression for estimating the impact of the six weather variables is given in Eq. 4 in 7.1. The black lines in Panel (e) and (f) indicate the estimated linear relationship between temperature and rice yield.⁹ The coefficient for temperature in JJAS is 0.016 and for temperature in ON -0.091 . Hence, an increase of temperature in ON by 1°C reduces the rice yield on average by 9.1%. Regarding rainfall (JJAS & ON) and the number of wet days (JJAS & ON), extrapolation is not a major concern since the future projections fall almost exclusively into the range of observations in the past.¹⁰ For example, only 0.2% of all future rainfall events (JJAS) projected in the SSP5-8.5 scenario exceed the observed maximum of 37mm. Further, given the flat slope of the rainfall bins, we assign the coefficient of the maximum in the past (37mm) for the 0.2% events exceeding past observations. The same procedure is applied to rainfall in ON. For the

⁸ Figs. 18 and 20 in 7.1 show that projected temperatures exceed past observations particularly by the end of the 21st century under the SSP5-8.5 scenario.

⁹ The estimates of the linear relationship are based on the unbinned temperature distribution, which results in a stronger weighting of more frequent observations.

¹⁰ For details see Figs. 15 in 7.1.

number of wet days there is no need for extrapolating values since all projected values are within the range of the past distribution of wet days¹¹

Climate Change Projections

Methodology

To quantify the impact of future climate change on agricultural yields in India, we retrieve the estimated $\hat{\beta}$ coefficients from the updated regression Eq. 4 and apply them to the data of each of the selected 8 climate models for the two different global warming scenarios (SSP1-2.6 and SSP5-8.5). Formally, we calculate the log of the predicted rice yield as follows:

$$\begin{aligned}
 \ln(\widehat{y_{it\bar{s}m}}) = & \underbrace{\sum_{a=1, a \neq \bar{a}}^{37} \widehat{\beta_a \text{rainfall}}_{a_{it\bar{s}m}} + \sum_{b=5, b \neq \bar{b}}^{125} \widehat{\beta_b \text{wetdays}}_{b_{it\bar{s}m}} + \widehat{\beta_c \text{temp}}_{it\bar{s}m}}_{\text{Monsoon (JJAS)}} \\
 & + \underbrace{\sum_{d=0, d \neq \bar{d}}^{20} \widehat{\beta_d \text{rainfall}}_{d_{it\bar{s}m}} + \sum_{e=0, e \neq \bar{e}}^{60} \widehat{\beta_e \text{wetdays}}_{e_{it\bar{s}m}} + \widehat{\beta_f \text{temp}}_{it\bar{s}m}}_{\text{Post Monsoon (ON)}} \\
 & + \underbrace{\hat{\alpha}_i + \widehat{\beta_5 \text{irrigation}}_{i_{t=2014}}}_{\text{District specific intercept (time-invariant)}}, \quad (2)
 \end{aligned}$$

where the notation is identical to Eq. 1 and complemented by the indices s and m , which denote the global warming scenario and the underlying climate model. Hence, $\ln(\widehat{y_{it\bar{s}m}})$ stands for the log of the predicted rice yield in district i in year t for the global warming scenario $s \in [SSP1 - 2.6, SSP5 - 8.5]$ as projected by climate model m . Note, that when quantifying the impact of climate change on agricultural output, we are interested in predicted changes in crop yield that are purely driven by changes of the climate in terms of average daily rainfall, number of wet days and average daily temperature. We implicitly ask the question on how would the rice yield change, if everything else remains equal expect the climate. Hence, the predicted changes in yield neglect possible adaptation strategies as well as technological progress in the future. Therefore, the calculation of the prediction consists of a time-varying part and a time-invariant part. The model projections of the *average daily rainfall* (JJAS & ON), the *average daily temperature* (JJAS & ON), as well as the *number of wet days* (JJAS & ON) constitute the time-varying part. The time-invariant part consists of an additive combination of the estimated district fixed effects $\hat{\alpha}_i$ and each district's irrigation share as of 2014. Thereby, we are able to separately predict for each of the 8 climate models the log of the rice yield for each individual year in our reference period (1995-2014), and for each year in the future period of 2021-2100 for both global warming scenarios. Lastly, we transform the log of the predicted rice yield back into the actual predicted rice yield ($\widehat{y_{it\bar{s}m}}$).

After having obtained $\widehat{y_{it\bar{s}m}}$, we calculate the relative differences between four future periods and our reference period. In order to identify heterogeneity over time, we split the future period 2021-2100 into four equal intervals comprising 20 years following the classification

¹¹ For details see Figs. 16 in 7.1.

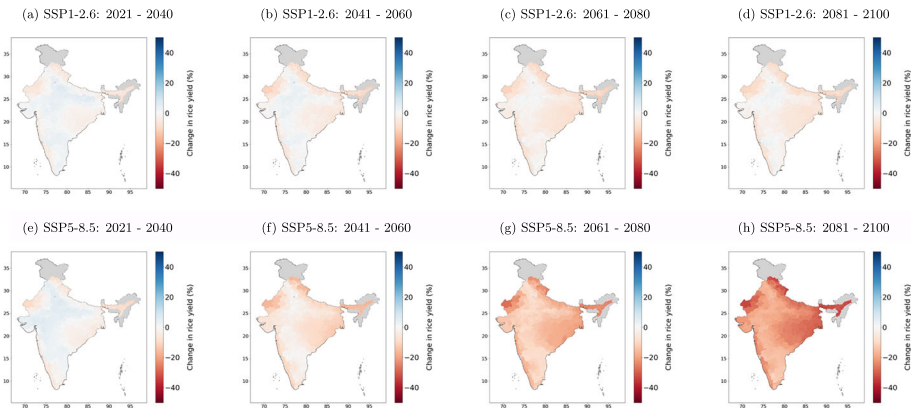


Fig. 2 Predicted rice yield changes. Figure 2 shows the predicted changes in rice yield (\hat{Y}) based on Eq. 3. Panel (a) - (d) display the predicted change in rice yield under SSP1-2.6 for the future periods relative to the reference period 1995-2014. Panel (e) - (f) show the predicted change in rice yield under SSP5-8.5. All predictions correspond to the average of the predictions of all 8 selected climate models. Data sources: ICRISAT, IMD, CMIP6

of the sixth Assessment Report of the IPCC (2022). The years 2021-2040 correspond to the short-term, 2041-2060 to the medium-term, 2061-2080 to the medium/long-term and 2081-2100 to the long-term future. We compare the predicted yield for these four future periods with our reference period covering the same number of years (1994-2014). Formally, the predicted relative changes in crop yield are calculated as follows:

$$\hat{Y}_{iTsm} = \frac{\sum_{t=T-19}^T \hat{y}_{itsm} - \sum_{t=1995}^{2014} \hat{y}_{itm}}{\sum_{t=1995}^{2014} \hat{y}_{itm}} \times 100, \text{ where } T \in [2040, 2060, 2080, 2100], \quad (3)$$

with \hat{Y}_{iTsm} standing for the predicted relative change (in %) in crop yield in district i in the future 20 year period $T \in [2040, 2060, 2080, 2100]$ for the global warming scenario $s \in [SSP1 - 2.6, SSP5 - 8.5]$ as projected by climate model m . In our main analysis we average the relative difference over all 8 climate models to account for general uncertainties across these models and to derive more robust tendencies of the climate projections.

Rice Yield Predictions

Following Eq. 3, we calculate the future change in rice yield under two different global warming scenarios. Figure 2 shows the results for all districts in our sample across India by time period (2021-2040, 2041-2060, 2061-2080, 2081-2100) and by global warming scenario (SSP1-2.6, SSP5-8.5).¹² The results for SSP1-2.6 are presented in Panels (a) - (d), while Panels (e) - (h) show the results for SSP5-8.5. Note that the results are averaged over all 8 climate models.¹³ While the predicted change in rice yield is similar in the short run (2021-2040) for both global warming scenarios, they strongly diverge in the long run. There is an average increase in rice yield of 0.18% for SSP1-2.6 and 0.31% for SSP5-8.5 in the short run relative to the reference period of 1995-2014. From the medium run onward the

¹² Figs. 7.1 - 30 in 7.1 shows the results for all other crops.

¹³ For the spatial distribution of changes in rice yields by the model-specific projections, see Figs. 22 and 23 in 7.1.

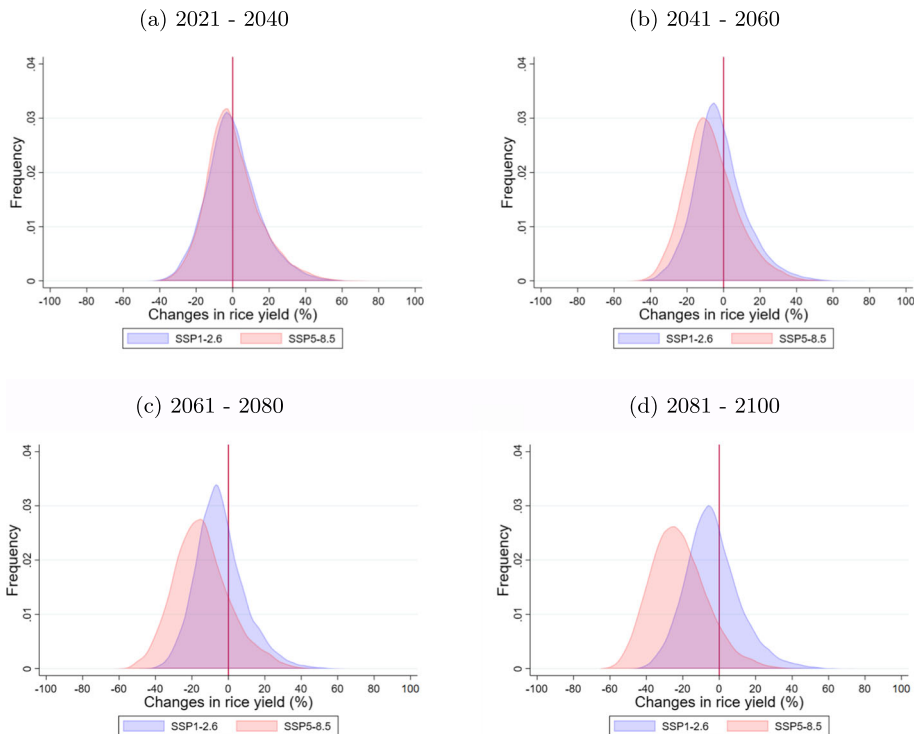


Fig. 3 Distribution of predicted rice yield changes. Figure 3 shows the distribution of predicted rice yield ($\hat{y}_{it,sm}$) based on Eq. 2 relative to the predicted mean rice yield of the reference period (1995–2014). Panel (a) depicts the distribution for the period of 2021–2040 compared to the reference period of 1995–2014 for rice. Panel (b)–(d) depict the distributions for the remaining periods. Blue color indicates the distribution under SSP1–2.6 and red color the distribution under SSP5–8.5. Data sources: Data sources: ICRISAT, IMD, CMIP6

predicted rice yield becomes negative for both scenarios. While the losses in the sustainable scenario remain moderate (–1.9%: 2041–2060; –4.2%: 2061–2080; –3.4%: 2081–2100), they further intensify in the worst case scenario (–6.8%: 2041–2060; –14.4%: 2061–2080; –22%: 2081–2100). In the long-term of the sustainable scenario, the average reduction in rice yield amounts to 3.4% relative to the reference period. For the worst case scenario, the predicted rice yield is expected to decrease on average by 22% relative to the reference period. When weighting the districts by their average rice production during the reference period, the long run reduction in rice yield amounts to 4.4% in the sustainable scenario and to 23% in the worst case scenario. Although the predicted impacts differ in magnitude across global warming scenarios, they follow a similar spatial pattern. The strongest negative impacts are expected in the northern and eastern regions. Impacts in the long-term for the sustainable scenario range from an increase of 3.2% in Mathura (Uttar Pradesh) to a decrease of 12.1% in North Cachar Hills (Assam). In the worst case scenario all districts are negatively affected, with Pithora Gar (Uttarakhand) having a predicted decrease in rice yield by 34% closely followed by North Cachar Hills with a decrease of 33.9%. With a predicted decrease of 11.5% Coimbatore in Tamil Nadu has the smallest decrease in the long run.¹⁴

¹⁴ For the annual moving averages of predicted rice yield relative to the reference period by SSP, see Figs. 31 in 7.1.

We translate the changes in rice yield into absolute changes relative to the average total production during the reference period. Midnapur district in West Bengal is the district with the strongest decrease in the long run for both scenarios. In the SSP1-2.6 scenario, the predicted decrease in rice production amounts to 160,550 tons and to 786,132 tons in the SSP5-8.5 scenario respectively. With an average total production of 2,611,352 tons during the reference period Midnapur district is also the district with the largest rice production during the reference period. In the long run, the aggregated absolute loss in rice production for all districts amounts to 4 mio. tons in the sustainable scenario and 21 mio. tons in the worst case scenario compared to 90 mio. tons during the reference period. For further details on the absolute changes in predicted rice yield see Figs. 21 in 7.1.

The entire distribution of all potential outcomes in predicted changes in annual rice yield as projected by the 8 different climate models is illustrated in Fig. 3. For the sustainable scenario, the share of years associated with a decrease in rice yield relative to the reference period increases from 52% in the short-run (2021–2040) to 62% in the long run (2081–2100). In the worst case scenario, the number of years with a decrease in rice yield increases from 53% in the period of 2021–2040 to 90% in the latest period of 2081–2100. Note however,

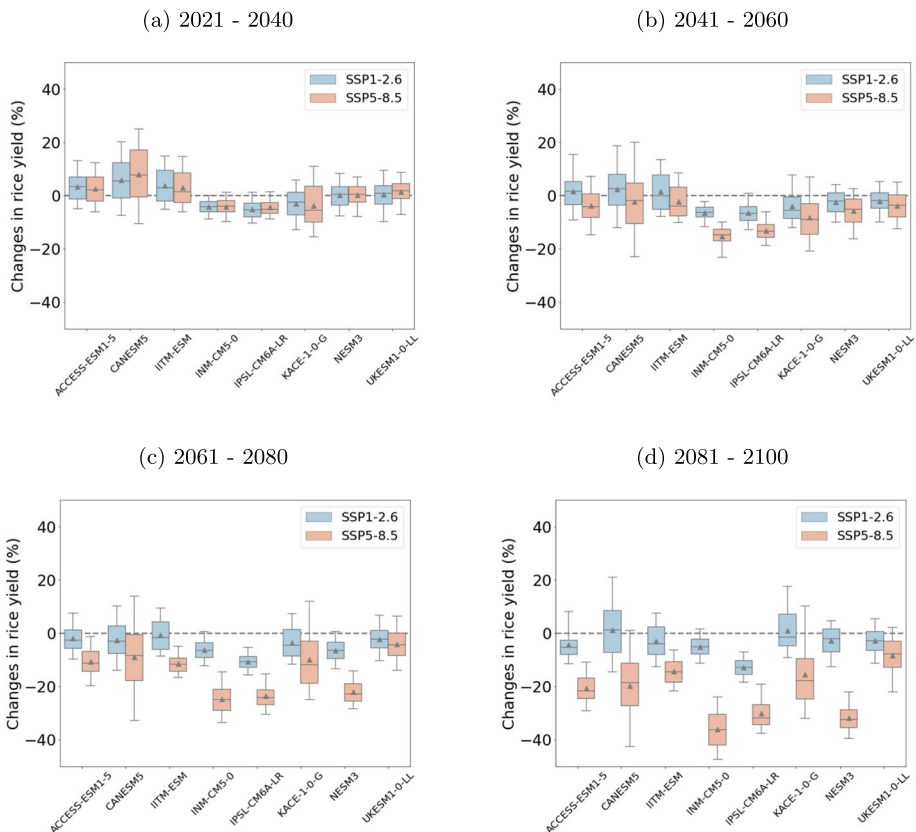


Fig. 4 Comparison across models. Figure 4 shows distribution of the predicted changes in yield (\hat{Y}) as predicted based on Eq. 3 across India for each climate model separately. Panel(a) depicts the results for the period of 2021–2040 compared to the reference period of 1995–2014, where blue boxplots display the results under SSP1-2,6 and red boxplots under SSP5-8.5. Triangles refer to the mean and the solid lines within the boxplots to the median. Panel (b) - (d) depict the results for the remaining periods. Data sources: ICRISAT, IMD, CMIP6

that while the means of the predicted changes in rice yield diverges across the SSPs, the variation around the mean does not differ systematically. Even in the long run, where strongest differences in weather realizations are expected, the difference in the standard deviation of the SSP1-2.6 and SSP5-8.5 scenario is minimal. The standard deviation for the SSP1-2.6 scenario equals 15.5 pp and for the SSP5-8.5 scenario 15.8 pp .

The general results on predicted changes in rice yield are averaged over the 8 selected climate models. Figure 4 depicts the results for each of the selected climate models separately and thereby provides insights into model-specific heterogeneity in the predicted impacts of climate change on the rice yield in India. As shown in Panel (a) of Fig. 4, there is no strong intra- and intermodel heterogeneity in predicted rice yield changes in the short-term. However, in the long-term, as shown in Panel (d), these differences become more pronounced. The average model-specific decreases in rice yield for the SSP5-8.5 scenario range from 36% (INM-CM5-0 model / Institute of Numerical Mathematics) to 8% (UKESM1-0-LL / Met Office Hadley Centre). For the sustainable SSP1-2.6 scenario, the IPSL-CM6A-LR model of the Institut Pierre Simon Laplace predicts the strongest decrease in the long-term amounting 12%. Two models (CANESM5 / Canadian Centre for Climate Modelling and Analysis and KACE-1-0-G / National Institute of Meteorological Sciences Korea) predict a slight positive increase in the long run under SSP1-2.6. The differences between the models are originated in the different implementation of physical processes and the parameterization schemes for sub-grid scale processes. Besides, this study only uses one simulation per model instead of using an ensemble of several simulations per model. Thus, the particular simulation might be on the upper or lower end if comparing with regard to their output for the relevant weather variables. Taking the multi-model mean of the 8 selected models, as done in this study, is an established way to reduce the effect of model-specific outcomes (Li 2015).

Turning to intra-model differences by global warming scenario, the UKESM1-0-LL model is associated with the lowest difference between the two scenarios (-3.2% in SSP1-2.6 vs -8% in SSP5-8.5). The most pronounced difference is projected by the INM-CM5-0 model, with an average decrease in rice yield in the SSP5-8.5 scenario of 31.2 pp lower than in the sustainable SSP1-2.6 scenario (-4.8% in SSP1-2.6 vs. -36% in SSP5-8.5).

Decomposition of Climate Change Impacts

In the following, we use our empirical approach to decompose the predicted changes by isolating the individual effects of each variable. We do this by looking at *ceteris paribus* changes. Put differently, we ask the question on how would the crop yield change if only one of the variables (e.g. rainfall in JJAS) changes over time and all other variables remain at the level of the reference period 1995–2014. Figure 5 shows the results of this decomposition for the long-term (2081–2100), since the aggregated changes are most pronounced for this period. Figures 32 – 34 in 7.1 contain the results for all other periods. If only the average daily rainfall during JJAS would change most of the crops would be positively affected by this change (except maize), see Panel (a) of Fig. 5. However, the extent of the changes are rather limited. Further, the general increase in the number of wet days during JJAS have a positive impact on the crop yields (Panel (c)). The results for *ceteris paribus* changes in rainfall and the number of wet days during ON suggest that these variables only have minor impact on the changes in crop yield (Panel (b) and (d)). In turn, the projected increases in temperature in JJAS and ON exert strong effects on the predicted rice yield. The small gains due to additional rainfall and number of wet days during JJAS are more than offset by the negative impact of temperature increases in ON. If only the temperature in ON would change

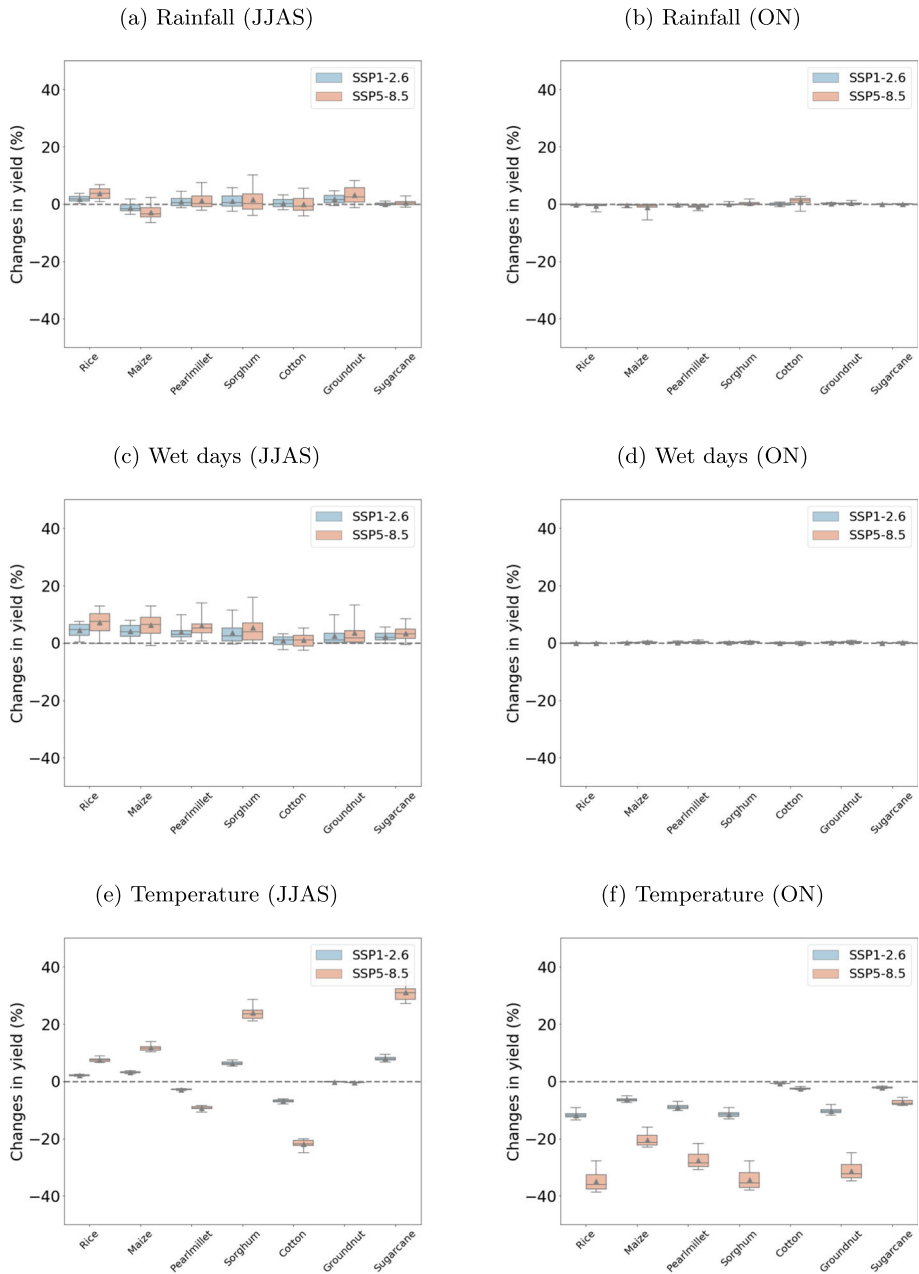


Fig. 5 Estimation results by variable (2081-2100). Figure 5 shows distribution of the predicted changes in yield (\hat{Y}) as predicted based on Eq. 3 across India for all crops and each variable separately. Panel(a) depicts the results for the period of 2081-2100 compared to the reference period of 1995-2014, when keeping all variables at the level of the reference period except rainfall (JJAS). Panel (b) - (d) depict the results for the remaining variables. Blue boxplots display the results under SSP1-2.6 and red boxplots under SSP5-8.5. Triangles refer to the mean and the solid lines within the boxplots to the median. Data sources: ICRISAT, IMD, CMIP6

and everything else would stay equal, the predicted rice yield in the long run would decrease on average by 12% (SSP1-2.6) and 35% (SSP5-8.5), respectively. Further, the main driving variable for the expected increase in sugarcane yield is the average daily temperature in JJAS.

Sensitivity and Adaptation Gap

The following section describes the sensitivity of our results with respect to temperature in ON, which is dominating the predicted changes in rice yield. In our results, the predicted changes in rice yield are calculated with the estimates obtained from Eq. 4, with the point estimate for temperature in ON corresponding to $\hat{\beta} = -0.091$ as depicted in Panel (f) of Fig. 1. In order to account for statistical uncertainty in our results, we recalculate the predicted changes in rice yield with respect to changes in the $\hat{\beta}$'s for temperature in ON. Put differently, we examine how the predicted rice yield changes, if we alter the slope of the the temperature effect in ON. Figure 6 illustrates how the results for rice yield respond to these marginal

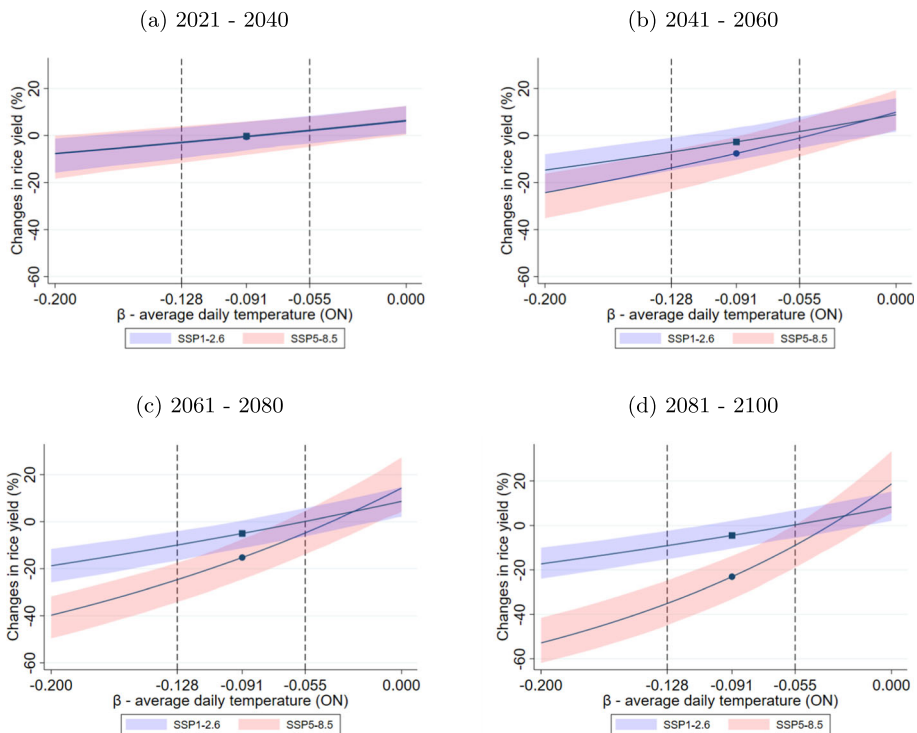


Fig. 6 Adaptation gap and sensitivity with respect to average daily temperature (ON). Figure 6 shows the predicted changes in rice yield (\hat{Y}) based on Eq. 3 relative to the underlying coefficient (β) for temperature in ON. Panel (a) plots the predicted changes in rice yield for the years 2021–2040 relative to the reference period 1995–2014. Panel (b) – (d) plots the predicted relative change in rice yield for the remaining periods. The dashed lines indicate the 95% confidence interval for temperature (ON) as estimated in Eq. 4. The circle and square display average predicted changes in rice yield when using the initial point estimate for temperature (ON) of -0.091. The blue-shaded and red-shaded area display the 95% range of of the district prediction under SSP1-2.6 and SSP5-8.5 respectively. Data sources: CMIP6 and author's calculations based on ICRISAT and IMD

changes in the estimated effect of temperature in ON with the x-axis indicating the $\hat{\beta}$ s and the y-axis the resulting rice yield predictions for every district. The dashed lines represent the 95% confidence interval of the estimated temperature effect, which ranges from -0.128 to -0.055 (and a point estimate of -0.091). Analogously to the box plots in the previous Figures, the blue-shaded area displays the 95%-bandwidth of the prediction results for the SSP1-2.6 scenario and the red-shaded area for the SSP5-8.5 scenario. The solid lines indicate averaged district-predictions across India, with the circle and the square marking our results when using the initial point estimate of -0.091 (Panel (d): -3.4% under SSP1-2.6 and -22% under SSP5-8.5). Using these two points as starting points for the sensitivity analysis and moving to the right on the x-axis would correspond to a flatter slope and a weakening of the temperature effect as compared to the initial results. Vice versa, moving to the left implies a steeper slope and a stronger negative effect of temperature in ON.¹⁵

A $\hat{\beta}$ of -0.055 , which corresponds to the the upper bound of the 95% confidence interval of the estimated temperature effect in ON, would lead to an average increase in rice yield of 1% in the long-term under the sustainable scenario. In the worst case scenario, the average rice yield would decrease on average by 8%. Hence, under the SSP5-8.5 scenario, even when assuming the weakest statistically supported impact of temperature in ON on rice yield, the negative impact of temperature in ON would still outweigh the positive gains of increasing rainfall and an increasing number of wet days. Assuming a $\hat{\beta}$ of -0.128 , which corresponds to the the lower bound of the 95% confidence interval of the estimated temperature effect in ON, rice yield would decrease on average by 8% in the SSP1-2.6 scenario. In the SSP5-8.5 scenario, the average decrease in rice yield would amount to 34%. Thus, assuming the strongest statistically supported negative relation of temperature in ON for the sustainable scenario (-0.128) provides the same results as when assuming the weakest statistical relation (-0.055) in the worst case scenario (both cases are associated with an 8% decrease in rice yield).

Finally, the sensitivity analysis provides implications in terms of adaption and mitigation. The reduction of the slope, which is equivalent to gradually reducing the negative impact of temperature in ON, can be interpreted as some form of successful adaptation against the negative temperature effects. The initial results for the sustainable SSP1-2.6 scenario, which projects the future climate in a world of successfully mitigating greenhouse gases, suggest an average decrease in rice yield by 3.4%. In the worst case scenario (SSP5-8.5) that is characterized by failed mitigation, one would need to cut the negative temperature effect in ON by around 50% (from -0.091 to -0.046) in the long run to reduce the average decrease in predicted rice yield from 22% to 3.4%, which corresponds to the predicted outcome of the SSP1-2.6 scenario. The decreasing tendency of agricultural yield is dominated by the temperature increase in ON. Yet, studies focusing adaption find only very limited possibilities for farmers to adapt against extreme heat in the past: By comparing long-difference estimates with short-difference estimates (Burke and Emerick 2016) conclude that even in a technologically advanced economy such as the US, the observed adaptation counteracting heat impacts has been very limited in the past. Wing et al. (2021) confirm theses findings at the global level. In the case of India, past adaptations have been focused on droughts given that the second half of the 21st century was dominated by the rainfall-reducing effect of aerosols on the Indian monsoon accompanied by increased occurrences of droughts (Seth

¹⁵ Note that the slope of the predictions is convex due to the log-linear relationship between rice yield and temperature in ON. 7.1 provides a more detailed explanation on the convexity of the slope.

2019). Hence, the incorporation of past adaptation efforts against droughts might not be meaningful for future global warming that is projected to be characterized by a simultaneous increase in rainfall and temperature and might therefore require different adaptation strategies. However, studies focusing on adaptation have come to the conclusion that adaptation has offset 9% of lost profits in India from 1956 to 1999 (Taraz Taraz). By adapting growing periods, approx. 5–15% of reduced impact are feasible in India (Minoli 2022). Aragon et al. (2021) find that short-term adjustment reactions of farmers include increasing the area planted and a change of crop mix. These and comparable adaptation mechanisms could be difficult to implement ex-ante, if the negative temperature effects only occur at the end of the growing season (ON), when planting decisions have been made already. Thus, the potential for adaptation is limited underlining the importance of mitigation.

Conclusion

The agricultural sector in India is highly dependent on the annual monsoon realizations. As projected by CMIP6 climate models, seasonal rainfall will increase due to global warming. In our study, we find that the positive effects associated with an increase in seasonal rainfall are insufficient to counteract the negative impacts resulting from an increase in local temperature. Overall, we show that agricultural yield is predicted to significantly decrease in the future, strongest in the worst case scenario. While the rice yield decreases on average by 22% relative to the years of 1994–2014 in the SSP5-8.5 scenario, the predicted decreases in rice yield amounts to 3.4% under the SSP1-2.6 scenario. This tendency holds for all major crops that are grown during the monsoon in India except for sugarcane. As Zhao (2016) report, statistical approaches as conducted in this study, have the tendency to quantify crop yield losses on the lower end of potential deficits compared to crop models and field warming experiments. Taking this into account, the negative anomalies might even be higher than quantified in this study. We further show that it is especially the northern and eastern regions in India that are associated with the largest decreases in agricultural yield. These results show that by mitigating climate change, the losses of rice yield in India as a result of climate change can be reduced from 22% to 3%. In the worst case scenario, when mitigation efforts were unsuccessful, one would need to reduce the negative impact of temperature in ON by 50% in order to reach the predicted outcome of the sustainable scenario. Hence, the results can serve as an indication of where to prioritize adaptation efforts.

While we control for general technological progress as observed in the past, the pressure created by future yield losses might lead to national-scale adaptation strategies (incl. technological progress) complemented by individual farmer decisions that exceed the previously observed adaptation efficiency. These adaptation measurements could include a shift towards climate resistant crops, a timely adaptation of growing periods or expanding the irrigation infrastructure. Nevertheless, it is particularly challenging to adapt to temperature changes (Taraz 2018) and studies revealed limited potential of adaptation measurements in India (Taraz Taraz; Minoli 2022). However, the increasing temperature in combination with a loss in biodiversity might lead to a probability of diseases and pests exceeding past observations. Additionally, it has to be noted that the CO_2 fertilization effect opposing the negative impact of increasing temperatures is not taken into account in our modelling approach. Future work could aim to incorporate these aspects.

A Appendix

Data

This section complements Section “Data” in the main paper. Table 2 contains additional descriptive statistics for all seven crops. Figure 7 plots the spatial distribution of the main weather indices as well as rice yield, rice production for the years 1966–2014 and rice irrigation for 2014. Figure 7 provides a detailed description of the climate model evaluation and selection process.

Table 2 Descriptive statistics all crops

	(1) <i>Mean</i>	(2) <i>SD</i>	(3) <i>Min</i>	(4) <i>Median</i>	(5) <i>Max</i>	(6) <i>N</i>	(7) <i>Source</i>
1966 - 2014							
Rice							
-Yield (kg/ha)	1,450	927.7	0	1,297	6,547	15,176	ICRISAT
-Production (1000tons)	217.7	315.0	0	93.97	3,153	15,176	ICRISAT
-Share irrigated area	0.441	0.399	0	0.336	1	15,176	ICRISAT
Sorghum							
-Yield (kg/ha)	575.1	544.8	0	534	6,531	15,158	ICRISAT
-Production (1000tons)	19.09	45.59	0	1.300	604.7	15,158	ICRISAT
-Share irrigated area	0.043	0.150	0	0	1	15,076	ICRISAT
Maize							
-Yield (kg/ha)	1,344	1,102	0	1,124	11,120	15,170	ICRISAT
-Production (1000tons)	32.95	72.54	0	5.900	1,028	15,170	ICRISAT
-Share irrigated area	0.192	0.305	0	0.0190	1	15,170	ICRISAT
Pearlmillet							
-Yield (kg/ha)	501.8	558.3	0	397	9,714	15,144	ICRISAT
-Production (1000tons)	21.72	58.13	0	0.300	826.8	15,172	ICRISAT
-Share irrigated area	0.056	0.165	0	0	1	15,125	ICRISAT
Cotton							
-Yield (kg/ha)	119.9	191.0	0	0	5,000	15,183	ICRISAT
-Production (1000tons)	6.675	23.55	0	0	376.6	15,188	ICRISAT
-Share irrigated area	0.180	0.330	0	0	1	15,124	ICRISAT
Groundnut							
-Yield (kg/ha)	745.2	600.7	0	761	8,500	15,188	ICRISAT
-Production (1000tons)	21.82	67.49	0	1.500	1,688	15,188	ICRISAT
-Share irrigated area	0.040	0.0991	0	0	1	15,188	ICRISAT
Sugarcane							
-Yield (kg/ha)	4,538	3,166	0	4,502	88,625	14,957	ICRISAT
-Production (1000tons)	74.13	188.8	0	8	2,005	14,957	ICRISAT
-Share irrigated area	0.681	0.421	0	0.975	1	14,957	ICRISAT

Notes: Sample consists of a panel of 313 districts for the years 1966–2014. District boundaries are drawn as of 1966. Sources for agricultural output from ICRISAT

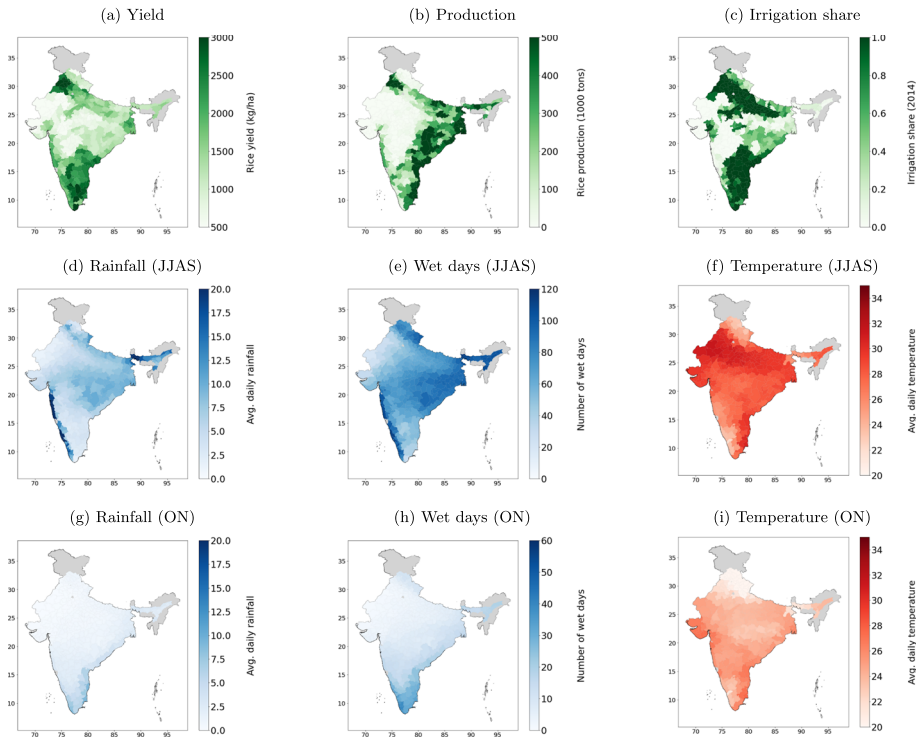


Fig. 7 Figure 7 plots the descriptive statistics of the main estimation sample as described in Section “Data”. Panel (a) plots the average rice yield for the years 1966–2014 in kg/ha. Panel (b) the average rice production in 1000t and Panel (c) the share of irrigated area as of 2014. Panel (d)–(i) plot average daily rainfall in mm/day, number of wet days (>0.1 mm) and average daily temperature (in $^{\circ}\text{C}$) for JJAS and ON. Data sources: ICRISAT, IMD

Climate Model Selection

In this study, we use the latest generation of general circulation models that participated in the Coupled Model Intercomparison Project phase 6 (CMIP6) and perform a detailed model evaluation in order to identify the models that are most suitable for our study i.e. perform best regarding the climate indices relevant for this study. The model evaluation is based on the IMD observational data and the reference period applied is 1966–2014. In order to select a reasonable number of climate models, we choose selection criteria that are commonly used in the context of climate model evaluations and regarding monsoon systems. The following criteria determine if the models are selected for the analysis in this study:

- The average rainfall during the summer monsoon season (JJAS) as well as the post season (ON) is within one standard deviation of the observed mean.
- The average temperature during the monsoon season (JJAS) as well as the post season (ON) is in the range of observed mean plus/minus 10%.
- The average number of wet days during the summer monsoon season (JJAS) and the post season (ON) is within plus/minus 35% of the observed.

Table 3 Overview of the 21 CMIP6 models

Modeling Center (Group)	CMIP6 Model	resolution (A/L/O) [km]
Commonwealth Scientific and Industrial Research Organisation (CSIRO)	ACCESS-ESM1-5	250/250/100
Alfred Wegener Institute (AWI)	AWI-CM-1-1-MR	100/100/25
Beijing Climate Center, China Meteorological Administration (BCC)	BCC-CSM2-MR	100/100/50
Chinese Academy of Meteorological Sciences (CAMS)	CAMS-CSM1-0	100/100/100
Canadian Centre for Climate Modelling and Analysis (CCCma)	CanESM5	500/500/100
National Center for Atmospheric Research (NCAR)	CESM2	100/100/100
Centre National de Recherches	CNRM-CM6-1	250/250/100
Météorologiques/ Centre Européen de Recherche et Formation Avancées en Calcul Scientifique (CNRM-CERFACS)	CNRM-ESM2-1	250/250/100
EC-Earth-Consortium	EC-Earth3	100/100/100
LASG, Institute of Atmospheric Physics, Chinese Academy of Sciences (CAS)	FGOALS-g3	250/250/100
NOAA Geophysical Fluid Dynamics Laboratory (NOAA-GFDL)	GFDL-ESM4	100/100/50
Centre for Climate Change Research (CCCR), Indian Institute of Tropical Meteorology (IITM)	IITM-ESM	250/250/100
Institute of Numerical Mathematics (INM)	INM-CM5-0	100/100/50
Institut Pierre Simon Laplace (IPSL)	IPSL-CM6A-LR	250/250/100
National Institute of Meteorological Sciences-Korea Met. Administration (NIMS-KMA)	KACE-1-0-G	250/250/100
Japan Agency for Marine-Earth Science and Technology/ Atmosphere and Ocean Research Institute, University of Tokyo (MIROC)	MIROC6	250/250/100
Max Planck Institute for Meteorology (MPI-M)	MPI-ESM1-2-HR	100/100/50
Meteorological Research Institute (MRI)	MRI-ESM2-0	100/100/100
Nanjing University of Information Science and Technol- ogy (NUIST)	NESM3	250/2.5/100
Ministry of Science and Technology (MOST), National Center for High-performance Computing (NCHC)	TAIESM1	100/100/100
Met Office Hadley Centre (MOHC)	UKESM1-0-LL	250/250/100

Notes: CMIP6 models with the corresponding Modeling center and the native grid resolution (Atmosphere/Land/Ocean)

The results for the individual models and quantitative details can be seen in Tables 4, 5, 6, 7, 8 and 9. Since the models have undergone bias-correction aiming at optimizing the data with regard to mean rainfall and temperature, the model results are similar for mean rainfall and temperature. On the other hand, the results for the number of wet days reveal a wider spread since the bias correction was not applied for this index. Thus, the model selection is particularly determined by the models' performance regarding wet days.

The average rainfall in India during the summer monsoon is according to observation in the range of 868.7 plus/minus 78.3mm. All of the 21 CMIP6 models are able to capture

Table 4 Average seasonal rainfall (JJAS)

Models	Mean (mm)	SD (mm)	RMSE (mm)	RMSE/tot
IMD observations	868.7	78.3	—	—
ACCESS-ESM1-5	800.7	264.6	226.9	0.261
AWI-CM-1-1-MR	868.1	94.7	218.3	0.251
BCC-CSM2-MR	841.7	88.0	215.9	0.249
CAMS-CSM1-0	878.1	83.1	217.2	0.250
CANESM5	821.2	263.4	219.6	0.253
CESM2	841.6	190.3	208.6	0.240
CNRM-CM6-1	849.1	118.7	215.9	0.249
CNRM-ESM2-1	836.7	138.4	217.2	0.250
EC-EARTH3	855.4	158.6	218.4	0.251
FGOALS-G3	850.4	214.9	215.9	0.249
GFDL-ESM4	839.3	133.2	219.6	0.253
IITM-ESM	863.2	128.3	217.2	0.250
INM-CM5-0	833.6	129.6	214.7	0.247
IPSL-CM6A-LR	852.2	123.3	219.6	0.253
KACE-1-0-G	850.3	267.8	214.7	0.247
MIROC6	847.8	101.8	213.5	0.246
MPI-ESM1-2-HR	878.2	131.2	222.0	0.256
MRI-ESM2-0	838.4	242.2	222.0	0.256
NESM3	870.7	124.5	218.4	0.251
TAIESM1	854.7	122.1	219.6	0.253
UKESM1-0-LL	839.1	249.3	217.2	0.250
multi-model-mean	848.1	160.4	217.3	0.251
multi-model-mean (best)	841.4	193.8	219.6	0.3

Notes: Evaluation of CMIP6 models results for average daily rainfall (June–September) in comparison to the IMD observations. Besides, the ensemble mean of all models as well as of the selected 8 models are given. Presented are the mean average seasonal rainfall for JJAS, the standard deviation (SD) as well as the absolute and relative root mean square error (RMSE)

Table 5 Number of wet days (JJAS)

Models	Mean	SD	RMSE	RMSE/tot
IMD observations	81.1	5.2	—	—
ACCESS-ESM1-5	53.5	7.1	32.4	0.400
AWI-CM-1-1-MR	47.3	4.9	38.0	0.469
BCC-CSM2-MR	47.7	3.9	37.7	0.465
CAMS-CSM1-0	49.4	4.5	36.0	0.444
CANESM5	53.0	6.7	33.0	0.407
CESM2	46.3	9.3	38.9	0.480
CNRM-CM6-1	47.1	6.4	38.0	0.469
CNRM-ESM2-1	45.1	7.4	40.1	0.494
EC-EARTH3	38.1	6.0	47.1	0.581
FGOALS-G3	49.4	6.1	36.5	0.450
GFDL-ESM4	46.6	6.6	38.7	0.477

Table 5 continued

Models	Mean	SD	RMSE	RMSE/tot
IITM-ESM	53.3	5.8	32.4	0.400
INM-CM5-0	57.8	5.5	28.2	0.348
IPSL-CM6A-LR	59.3	7.5	26.9	0.332
KACE-1-0-G	53.2	10.1	32.3	0.398
MIROC6	45.6	5.2	39.5	0.487
MPI-ESM1-2-HR	48.9	5.7	36.7	0.453
MRI-ESM2-0	47.2	8.6	37.9	0.467
fNesm3	55.4	5.5	30.2	0.372
TAIESM1	46.6	6.6	38.7	0.477
UKESM1-0-LL	53.0	9.7	32.7	0.403
multi-model-mean	49.7	6.6	35.8	0.441
multi-model-mean (best)	54.8	7.2	31.0	0.382

Notes: CMIP6 evaluation results for the number of wet days (June–September) in comparison to the IMD observations. Besides, the ensemble mean of all models as well as of the selected 8 models are given. Presented are the average number of wet days for JJAS, its standard deviation (SD) as well as its absolute and relative root mean square error (RMSE)

Table 6 Average daily temperature (JJAS)

Models	Mean (°C)	SD (°C)	RMSE (°C)	RMSE/tot
IMD observations	27.82	0.45	—	—
ACCESS-ESM1-5	26.61	0.43	4.54	0.163
AWI-CM-1-1-MR	26.63	0.40	4.53	0.163
BCC-CSM2-MR	26.62	0.28	4.56	0.164
CAMS-CSM1-0	26.61	0.34	4.51	0.162
CANESM5	26.52	0.62	4.68	0.168
CESM2	26.71	0.48	4.52	0.162
CNRM-CM6-1	26.63	0.37	4.52	0.162
CNRM-ESM2-1	26.70	0.40	4.54	0.163
EC-EARTH3	26.54	0.39	4.58	0.165
FGOALS-G3	26.67	0.29	4.56	0.164
GFDL-ESM4	26.64	0.37	4.56	0.164
IITM-ESM	26.59	0.47	4.53	0.163
INM-CM5-0	26.60	0.39	4.51	0.162
IPSL-CM6A-LR	26.60	0.48	4.55	0.164
KACE-1-0-G	26.56	0.36	4.54	0.163
MIROC6	26.71	0.42	4.49	0.161
MPI-ESM1-2-HR	26.56	0.37	4.51	0.162
MRI-ESM2-0	26.60	0.38	4.57	0.164
NESM3	26.65	0.32	4.53	0.163
TAIESM1	26.72	0.44	4.55	0.164

Table 6 continued

Models	Mean (°C)	SD (°C)	RMSE (°C)	RMSE/tot
UKESM1-0-LL	26.64	0.38	4.55	0.164
multi-model-mean	26.62	0.40	4.54	0.163
multi-model-mean (best)	26.6	0.4	4.6	0.2

Notes: CMIP6 evaluation results for average daily temperature (June–September) in comparison to the IMD observations. Besides, the ensemble mean of all models as well as of the selected 8 models are given. Presented are the average daily temperature for JJAS, its standard deviation (SD) as well as its absolute and relative root mean square error (RMSE)

the mean rainfall within the range of plus/minus one standard deviation. The multi-model mean is 848.7mm for the 21 models and 841.4mm for the selected 8 models with best monsoon performance. These remarkably good results for rainfall simulation data are a

Table 7 Average rainfall (ON)

Models	Mean (mm)	SD (mm)	RMSE (mm)	RMSE/tot
IMD observations	108.0	26.4	—	—
ACCESS-ESM1-5	108.9	52.8	29.0	0.261
AWI-CM-1-1-MR	109.0	37.9	30.5	0.282
BCC-CSM2-MR	98.3	37.8	26.8	0.248
CAMS-CSM1-0	110.9	40.2	29.0	0.269
CANESM5	107.5	29.8	27.4	0.254
CESM2	102.8	42.8	26.9	0.249
CNRM-CM6-1	107.0	40.8	26.4	0.244
CNRM-ESM2-1	102.1	40.7	26.7	0.247
EC-EARTH3	105.5	44.9	24.8	0.230
FGOALS-G3	108.7	46.7	27.4	0.254
GFDL-ESM4	102.6	39.3	27.5	0.255
IITM-ESM	105.5	50.2	27.3	0.253
INM-CM5-0	106.0	51.5	26.7	0.247
IPSL-CM6A-LR	110.5	30.4	29.0	0.269
KACE-1-0-G	112.4	50.1	29.3	0.271
MIROC6	100.6	45.6	29.7	0.275
MPI-ESM1-2-HR	102.9	46.1	27.2	0.252
MRI-ESM2-0	101.2	45.0	28.5	0.264
NESM3	109.9	33.7	30.7	0.284
TAIESM1	105.4	33.5	27.0	0.250
UKESM1-0-LL	103.7	48.2	26.1	0.242
multi-model-mean	105.8	42.3	27.8	0.257
multi-model-mean (best)	108.1	43.3	28.2	0.261

Notes: CMIP6 evaluation results for average daily rainfall (October–November) in comparison to the IMD observations. Besides, the ensemble mean of all models as well as of the selected 8 models are given. Presented are the average daily rainfall (ON), its standard deviation (SD) as well as its absolute and relative root mean square error (RMSE)

Table 8 Number of wet days (ON)

Models	Mean	SD	RMSE	RMSE/tot
IMD observations	14.0	3.0	—	—
ACCESS-ESM1-5	10.2	2.4	6.7	0.479
AWI-CM-1-1-MR	9.0	2.5	7.8	0.557
BCC-CSM2-MR	8.4	2.0	8.1	0.579
CAMS-CSM1-0	9.3	2.7	8.3	0.593
CANESM5	12.4	2.5	4.7	0.336
CESM2	7.7	2.5	8.8	0.629
CNRM-CM6-1	8.8	2.4	7.8	0.557
CNRM-ESM2-1	8.3	2.6	8.0	0.571
EC-EARTH3	6.0	2.2	10.6	0.757
FGOALS-G3	9.9	2.8	7.4	0.529
GFDL-ESM4	8.2	2.2	8.4	0.600
IITM-ESM	9.2	2.4	8.0	0.571
INM-CM5-0	9.9	3.5	6.7	0.479
IPSL-CM6A-LR	11.2	2.8	5.3	0.379
KACE-1-0-G	10.1	3.0	7.3	0.521
MIROC6	7.7	2.1	9.3	0.664
MPI-ESM1-2-HR	8.7	2.4	7.9	0.564
MRI-ESM2-0	8.2	2.3	8.3	0.593
NESM3	11.3	3.3	5.7	0.407
TAIESM1	8.5	2.4	8.6	0.614
UKESM1-0-LL	10.2	2.7	6.9	0.493
multi-model-mean	9.2	2.6	7.6	0.543
multi-model-mean (best)	10.6	2.8	6.4	0.457

Notes: CMIP6 evaluation results for the number of wet days (October–November) in comparison to the IMD observations. Besides, the ensemble mean of all models as well as of the selected 8 models are given. Presented are the number of wet day (ON), its standard deviation (SD) as well as its absolute and relative root mean square error (RMSE)

result of the bias-correction. The not bias-corrected CMIP6 models have a general tendency to underestimate the observed mean (authornam [2021](#)).

The results for the average temperature during the summer monsoon season in India are revealing a negative bias of 1.2°C compared to the the IMD mean for June to September of 27.8 plus/minus 0.4°C (multi-model mean for the 21 CMIP6 models: 26.6°C and for the 8 models with best performance also: 26.6°C). This bias is a result of the different reference data that was applied in the context of the bias correction and the data basis for the model evaluation in this study: While the bias correction optimizes the data with regard to the W5E5 reanalysis data (Lange [2019](#)), we use the IMD data in this study for the model evaluation. The W5E5 data set has been created on the basis of 0.5° aggregated ERA5 reanalysis data (Hersbach [2020](#)) in combination with the WFDE5 dataset (WATCH Forcing data methodology applied to ERA5 reanalysis data; (Cucchi [2020](#); Weedon [2010](#))) as well as the precipitation data from version 2.3 of the Global Precipitation Climatology Project (GPCP, (Adler [2003](#))). The reason for the strong difference in mean temperature in the W5E5 reanalysis data set and the IMD observation data set must result from the difference in the

Table 9 Average daily temperature (ON)

Models	Mean (°C)	SD (°C)	RMSE (°C)	RMSE/tot
IMD observations	23.76	0.54	—	—
ACCESS-ESM1-5	22.09	0.42	5.27	0.222
AWI-CM-1-1-MR	22.11	0.47	5.25	0.221
BCC-CSM2-MR	22.22	0.44	5.23	0.220
CAMS-CSM1-0	22.13	0.40	5.22	0.220
CANESM5	22.03	0.70	5.29	0.223
CESM2	22.22	0.63	5.24	0.221
CNRM-CM6-1	22.07	0.50	5.25	0.221
CNRM-ESM2-1	22.21	0.53	5.26	0.221
EC-EARTH3	22.09	0.65	5.27	0.222
FGOALS-G3	22.12	0.45	5.23	0.220
GFDL-ESM4	22.18	0.57	5.25	0.221
IITM-ESM	22.18	0.50	5.23	0.220
INM-CM5-0	22.12	0.39	5.20	0.219
IPSL-CM6A-LR	22.08	0.54	5.26	0.221
KACE-1-0-G	22.05	0.48	5.24	0.221
MIROC6	22.18	0.49	5.22	0.220
MPI-ESM1-2-HR	22.10	0.48	5.25	0.221
MRI-ESM2-0	22.22	0.51	5.28	0.222
NESM3	22.16	0.39	5.21	0.219
TAIESM1	22.08	0.55	5.30	0.223
UKESM1-0-LL	22.17	0.47	5.23	0.220
multi-model-mean	22.13	0.48	5.25	0.221
multi-model-mean (best)	22.11	0.49	5.24	0.221

Notes: CMIP6 evaluation results for average daily temperature (October–November) in comparison to the IMD observations. Besides, the ensemble mean of all models as well as of the selected 8 models are given. Presented are the average daily temperature (ON), its standard deviation (SD) as well as its absolute and relative root mean square error (RMSE)

methods applied in order to obtain the temperature data set. However, note that in our analysis we are interested in changes over time within climate projections. Hence, a general and time consistent underestimation of the number of wet days and temperature does not impact our results.

Regarding the number of wet days, the CMIP6 models clearly tend to underestimate the number of rainfall days compared to the historic mean of 1966–2014. Only 8 models are able to capture the number of wet days within the range of the average number of observed wet days of 81.1 plus/minus 35%. The 21 CMIP6 models reveal on average 49.8 days, while the multi-model mean is 54.8 wet days and thus closer to the observed mean when only the models that fulfill the selection criteria are chosen. Again by comparing two time periods, a time consistent bias cancels. Finally, the following 8 models fulfill the listed selection criteria: ACCESS-ESM1-5, CANESM5, IITM-ESM, INM-CM5-0, IPSL-CM6A-LR, KACE-1-0-G, NESM3, UKESM1-0-LL.

Empirical Approach

This section complements Section “[Empirical Approach](#)” in the main paper. Figure 8 summarizes our approach. Equation 4 provides the updated regression approach with the temperature bins replaced by a linear term. Figures 9, 10, 11, 12, 13 and 14 show the estimated coefficients of the weather variables for the respective crop yield.

$$\begin{aligned}
 \ln(y_{it}) = & \underbrace{\sum_{a=1, a \neq \bar{a}}^{37} \beta_a \text{rainfall}_{a_{it}} + \sum_{b=5, b \neq \bar{b}}^{121} \beta_b \text{wetdays}_{b_{it}} + \beta_c \text{temp}_{it}}_{\text{Monsoon (JJAS)}} \\
 & + \underbrace{\sum_{d=0, d \neq \bar{d}}^{20} \beta_d \text{rainfall}_{d_{it}} + \sum_{e=0, e \neq \bar{e}}^{57} \beta_e \text{wetdays}_{e_{it}} + \beta_f \text{temp}_{it}}_{\text{Post Monsoon (ON)}} \\
 & + \beta_5 \text{irrigation}_{it} + \alpha_i + \gamma_t + \epsilon_{it},
 \end{aligned} \tag{4}$$

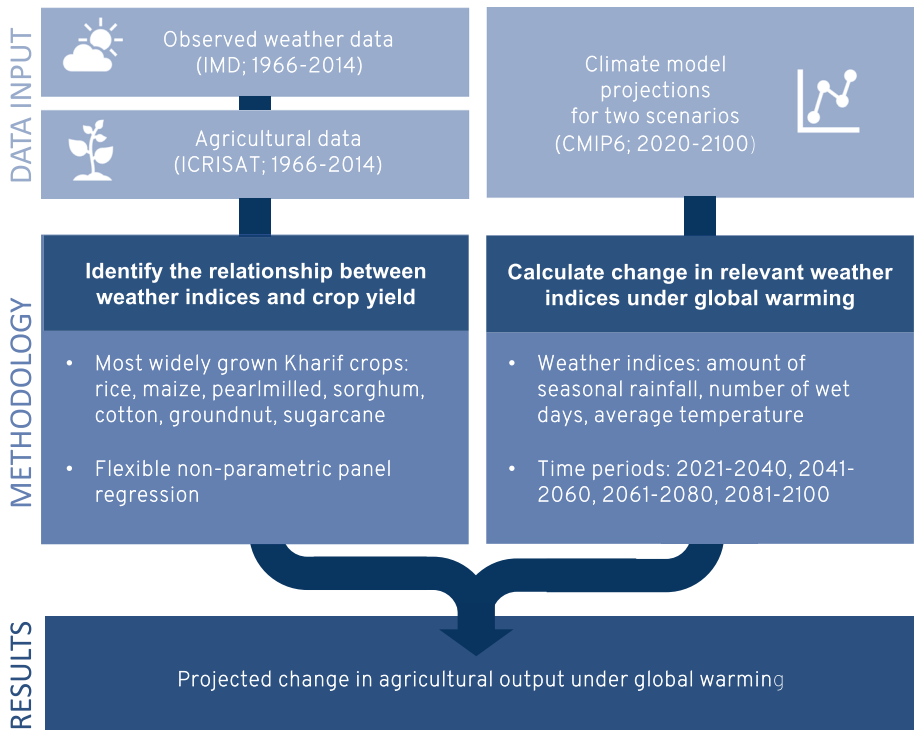


Fig. 8 This figure visualizes the input data, the working procedure and the output

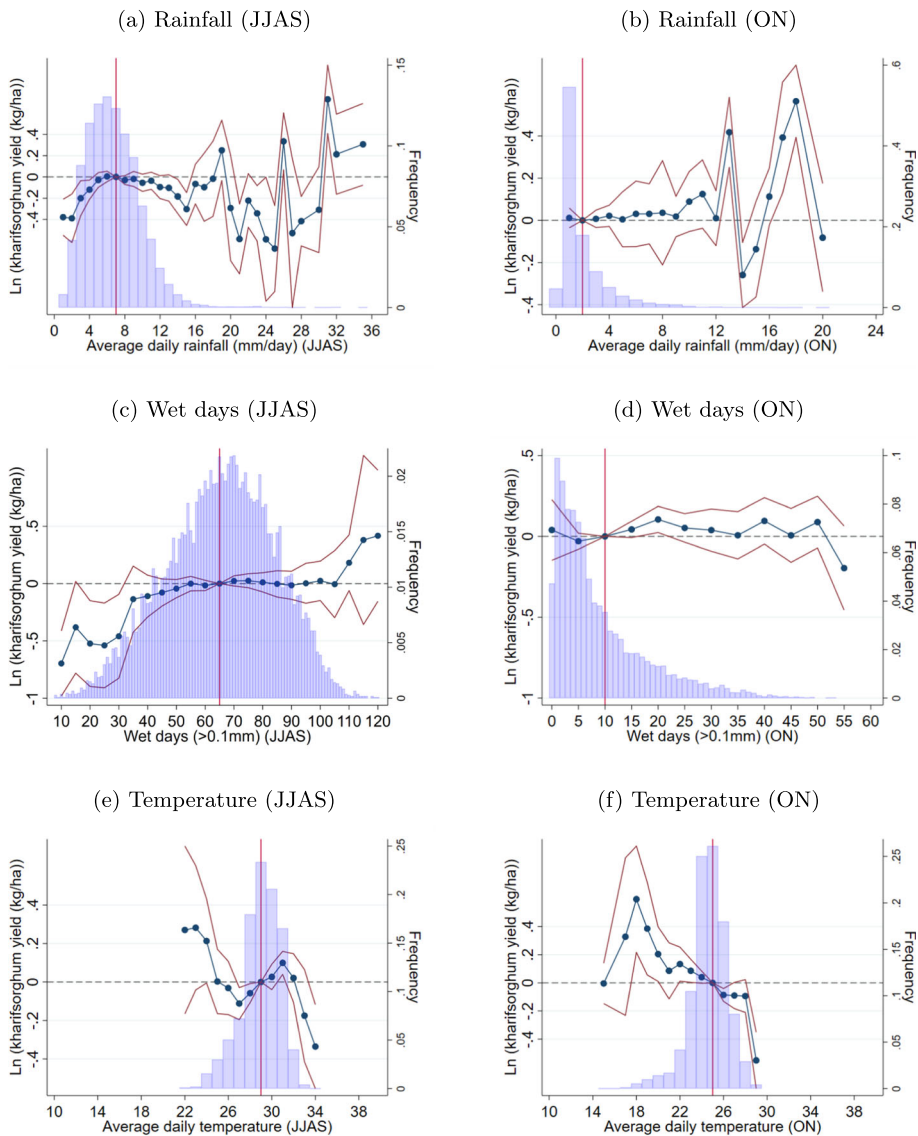


Fig. 9 Estimation results for sorghum. The plotted coefficients refer to the coefficients $\hat{\beta}$ as estimated according to Eq. 1. Red lines indicate the respective 95% confidence interval. The vertical red line refers to the omitted bin, which corresponds to the sample mean. Panel (a) depicts the results for average daily rainfall for the months of June, July, August and September (JJAS) on sorghum yield. Panel (b) - (f) depict the results for the remaining variables. Standard errors are clustered at the state level. The regression further includes district and year fixed effects, which are not reported. The blue colored bars display the binned distribution of the respective variables based on the the years 1966–2014. Data sources: ICRISAT, IMD, CMIP6

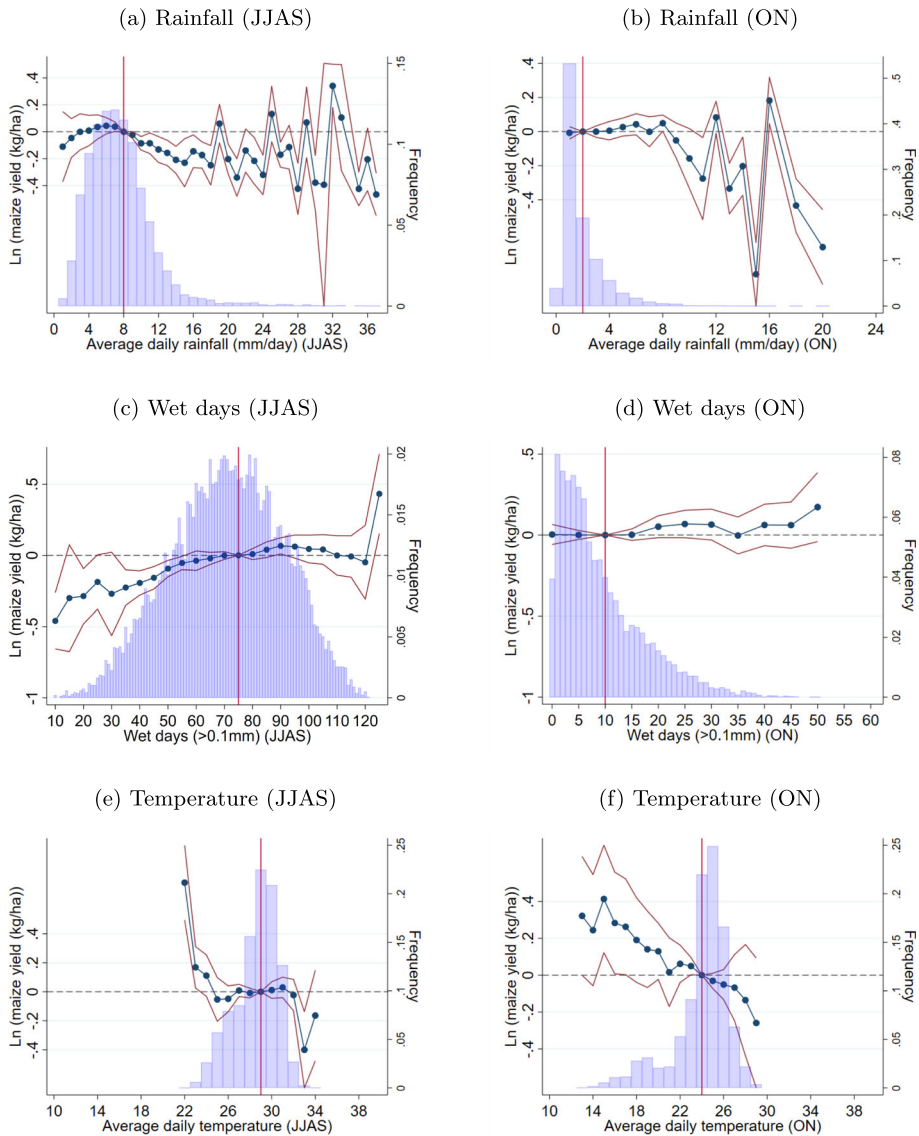


Fig. 10 Estimation results for maize. The plotted coefficients refer to the coefficients $\hat{\beta}$ as estimated according to Eq. 1. Red lines indicate the respective 95% confidence interval. The vertical red line refers to the omitted bin, which corresponds to the sample mean. Panel (a) depicts the results for average daily rainfall for the months of June, July, August and September (JJAS) on maize yield. Panel (b) - (f) depict the results for the remaining variables. Standard errors are clustered at the state level. The regression further includes district and year fixed effects, which are not reported. The blue colored bars display the binned distribution of the respective variables based on the the years 1966-2014. Data sources: ICRISAT, IMD, CMIP6

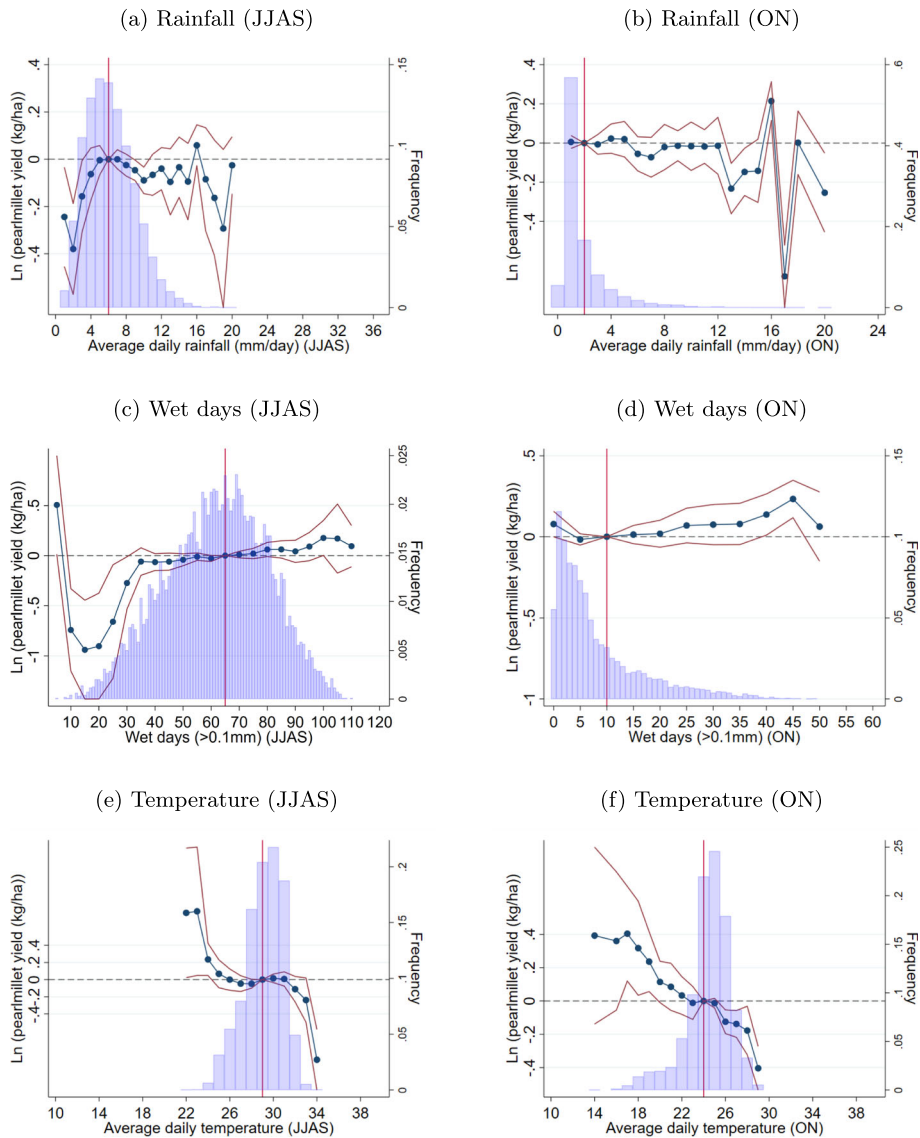


Fig. 11 Estimation results for pearl millet. The plotted coefficients refer to the coefficients $\hat{\beta}$ as estimated according to Eq. 1. Red lines indicate the respective 95% confidence interval. The vertical red line refers to the omitted bin, which corresponds to the sample mean. Panel (a) depicts the results for average daily rainfall for the months of June, July, August and September (JJAS) on pearl millet yield. Panel (b) - (f) depict the results for the remaining variables. Standard errors are clustered at the state level. The regression further includes district and year fixed effects, which are not reported. The blue colored bars display the binned distribution of the respective variables based on the the years 1966-2014. Data sources: ICRISAT, IMD, CMIP6

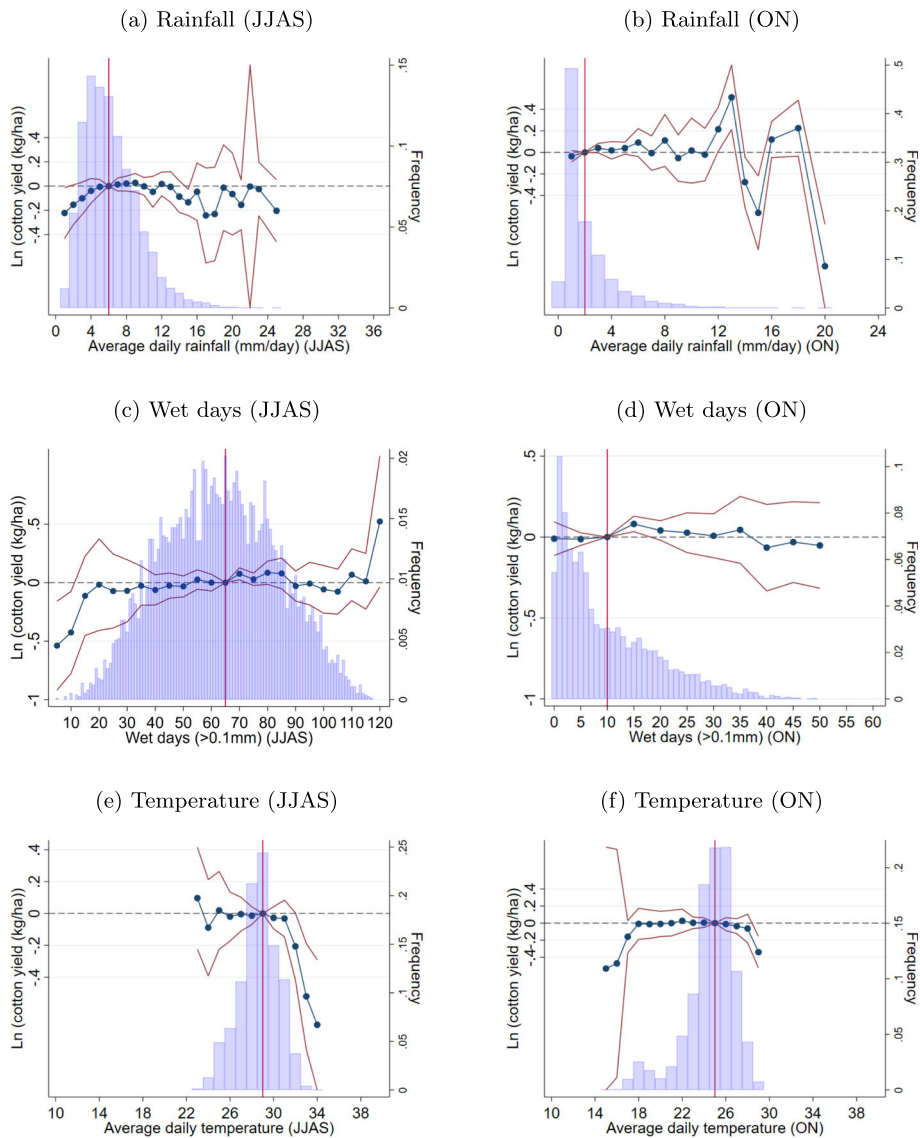


Fig. 12 Estimation results for cotton. The plotted coefficients refer to the coefficients $\hat{\beta}$ as estimated according to Eq. 1. Red lines indicate the respective 95% confidence interval. The vertical red line refers to the omitted bin, which corresponds to the sample mean. Panel (a) depicts the results for average daily rainfall for the months of June, July, August and September (JJAS) on cotton yield. Panel (b) - (f) depict the results for the remaining variables. Standard errors are clustered at the state level. The regression further includes district and year fixed effects, which are not reported. The blue colored bars display the binned distribution of the respective variables based on the the years 1966-2014. Data sources: ICRISAT, IMD, CMIP6

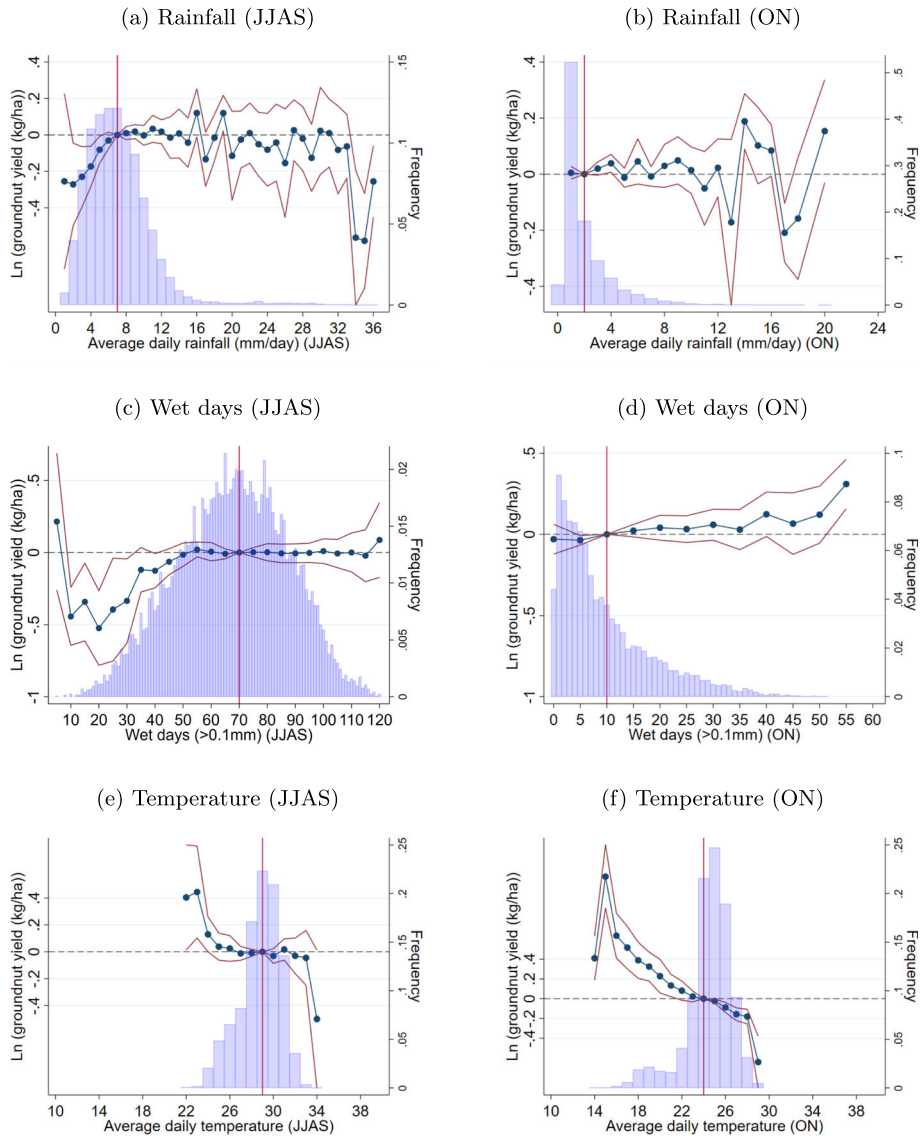


Fig. 13 Estimation results for groundnut. The plotted coefficients refer to the coefficients $\hat{\beta}$ as estimated according to Eq. 1. Red lines indicate the respective 95% confidence interval. The vertical red line refers to the omitted bin, which corresponds to the sample mean. Panel (a) depicts the results for average daily rainfall for the months of June, July, August and September (JJAS) on groundnut yield. Panel (b) - (f) depict the results for the remaining variables. Standard errors are clustered at the state level. The regression further includes district and year fixed effects, which are not reported. The blue colored bars display the binned distribution of the respective variables based on the years 1966–2014. Data sources: ICRISAT, IMD, CMIP6

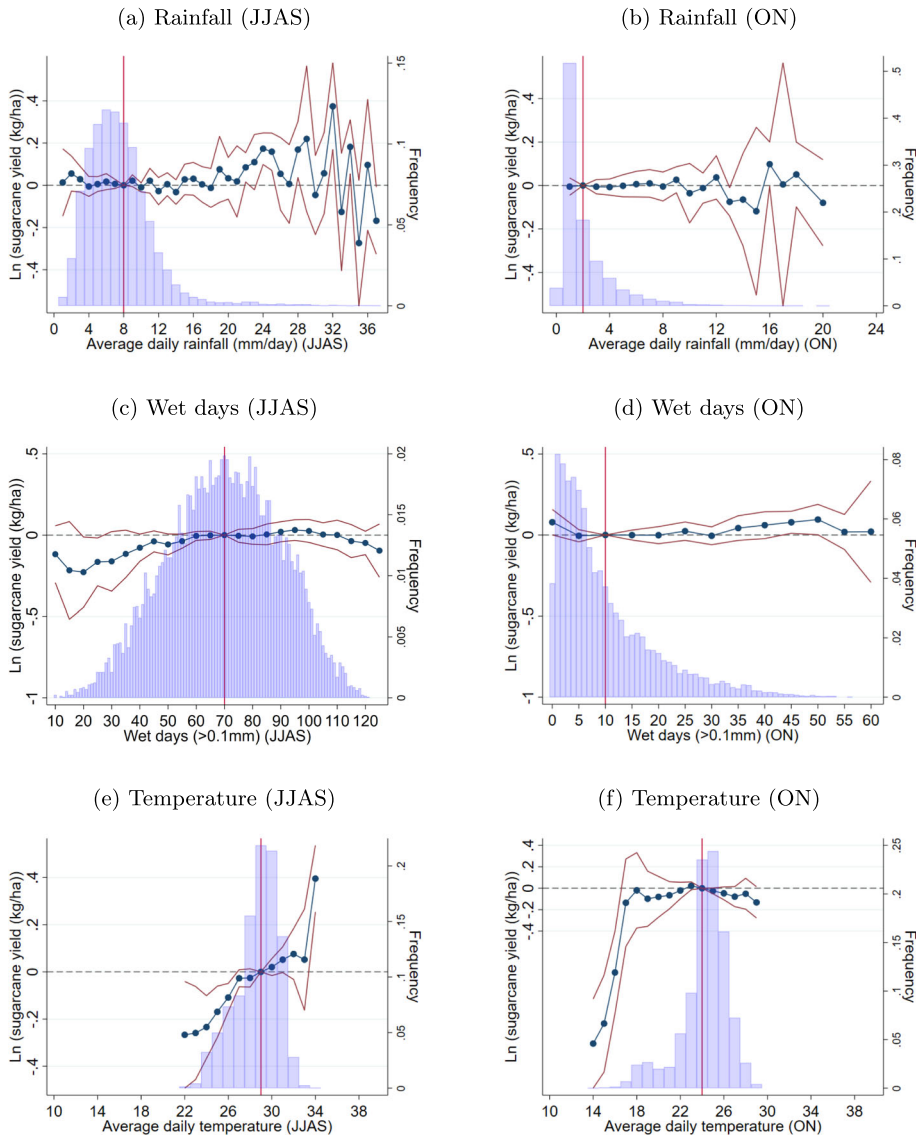


Fig. 14 Estimation results for sugarcane. The plotted coefficients refer to the coefficients $\hat{\beta}$ as estimated according to Eq. 1. Red lines indicate the respective 95% confidence interval. The vertical red line refers to the omitted bin, which corresponds to the sample mean. Panel (a) depicts the results for average daily rainfall for the months of June, July, August and September (JJAS) on sugarcane yield. Panel (b) - (f) depict the results for the remaining variables. Standard errors are clustered at the state level. The regression further includes district and year fixed effects, which are not reported. The blue colored bars display the binned distribution of the respective variables based on the years 1966-2014. Data sources: ICRISAT, IMD, CMIP6

Prediction

This section complements Section “Climate Change Projections” in the main paper. Figures 15, 16, 17, 18, 19 and 20 show the coefficients of the weather variables for rice yield and

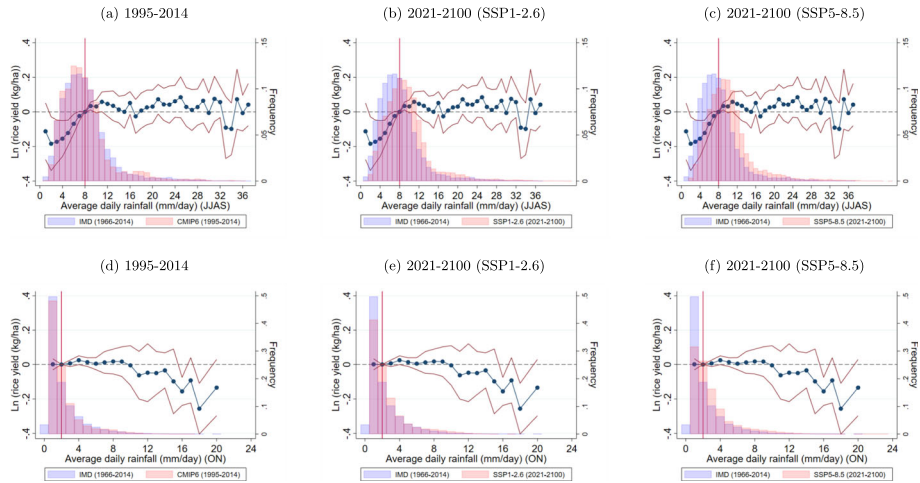


Fig. 15 Estimation results for rice and projected average rainfall (JJAS & ON) distributions. Figure 15 shows the plotted coefficients refer to the coefficients $\hat{\beta}$ as estimated according to Eq. 1. Red lines indicate the respective 95% confidence interval. The vertical red line refers to the omitted bin, which corresponds to the sample mean. All Panels display the results for the average daily rainfall for the months of June, July, August and September (JJAS) and October and November (ON) on rice yield. Standard errors are clustered at the state level. The regression further includes district and year fixed effects, which are not reported. The blue colored bars display the binned distribution of the respective variables based on the years 1966-2014. Panel (a) depicts the projected wet days (JJAS) distribution for the reference period. Panel (b) - (e) depict the projections for the future periods under under SSP1-2.6. Data sources: ICRISAT, IMD, CMIP6

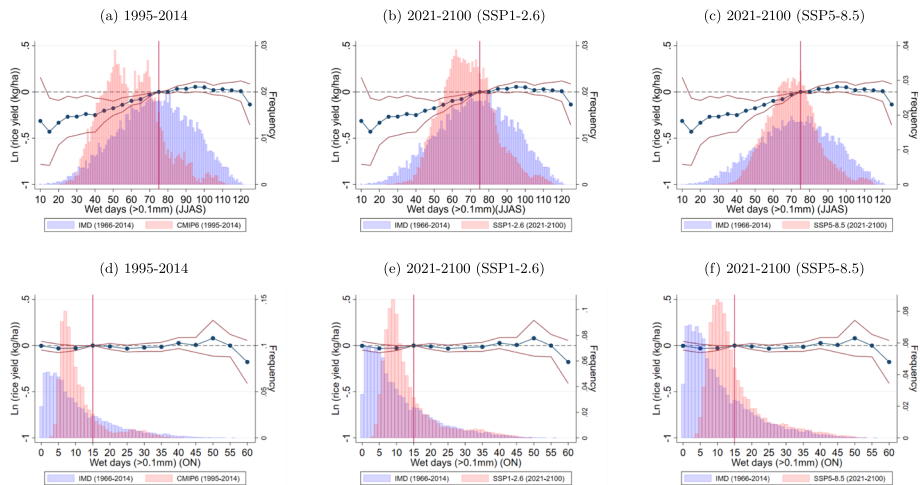


Fig. 16 Estimation results for rice and projected number of wet days (JJAS & ON) distributions. Figure 16 shows the plotted coefficients refer to the coefficients $\hat{\beta}$ as estimated according to Eq. 1. Red lines indicate the respective 95% confidence interval. The vertical red line refers to the omitted bin, which corresponds to the sample mean. All Panels display the results for the number of wet days for the months of June, July, August and September (JJAS) and October and November (ON) on rice yield. Standard errors are clustered at the state level. The regression further includes district and year fixed effects, which are not reported. The blue colored bars display the binned distribution of the respective variables based on the years 1966-2014. Panel (a) depicts the projected wet days (JJAS) distribution for the reference period. Panel (b) - (e) depict the projections for the future periods under under SSP1-2.6. Data sources: ICRISAT, IMD, CMIP6

the respective projections in order to calculate the predicted rice yield under SSP1-2.6 and SSP5-8.5.

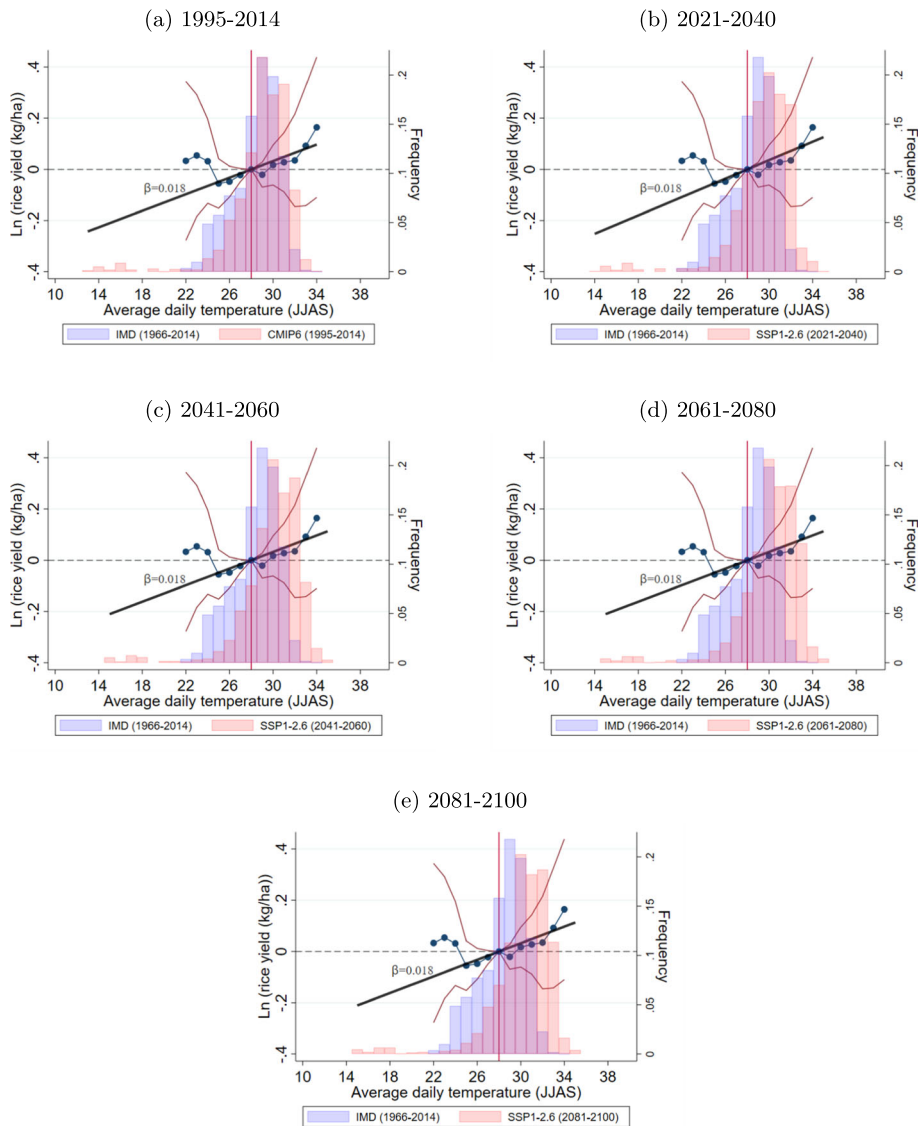


Fig. 17 Estimation results for rice and projected average temperature (JJAS) distributions (SSP1-2.6). The plotted coefficients refer to the coefficients $\hat{\beta}$ as estimated according to Eq. 1. Red lines indicate the respective 95% confidence interval. The vertical red line refers to the omitted bin, which corresponds to the sample mean. All Panels display the results for average daily temperature for the months of June, July, August and September (JJAS) on rice yield. Standard errors are clustered at the state level. The regression further includes district and year fixed effects, which are not reported. The blue colored bars display the binned distribution of the respective variables based on the years 1966-2014. Panel (a) depicts the projected temperature (JJAS) distribution for the reference period. Panel (b) - (e) depict the projections for the future periods under SSP1-2.6. Data sources: ICRISAT, IMD, CMIP6

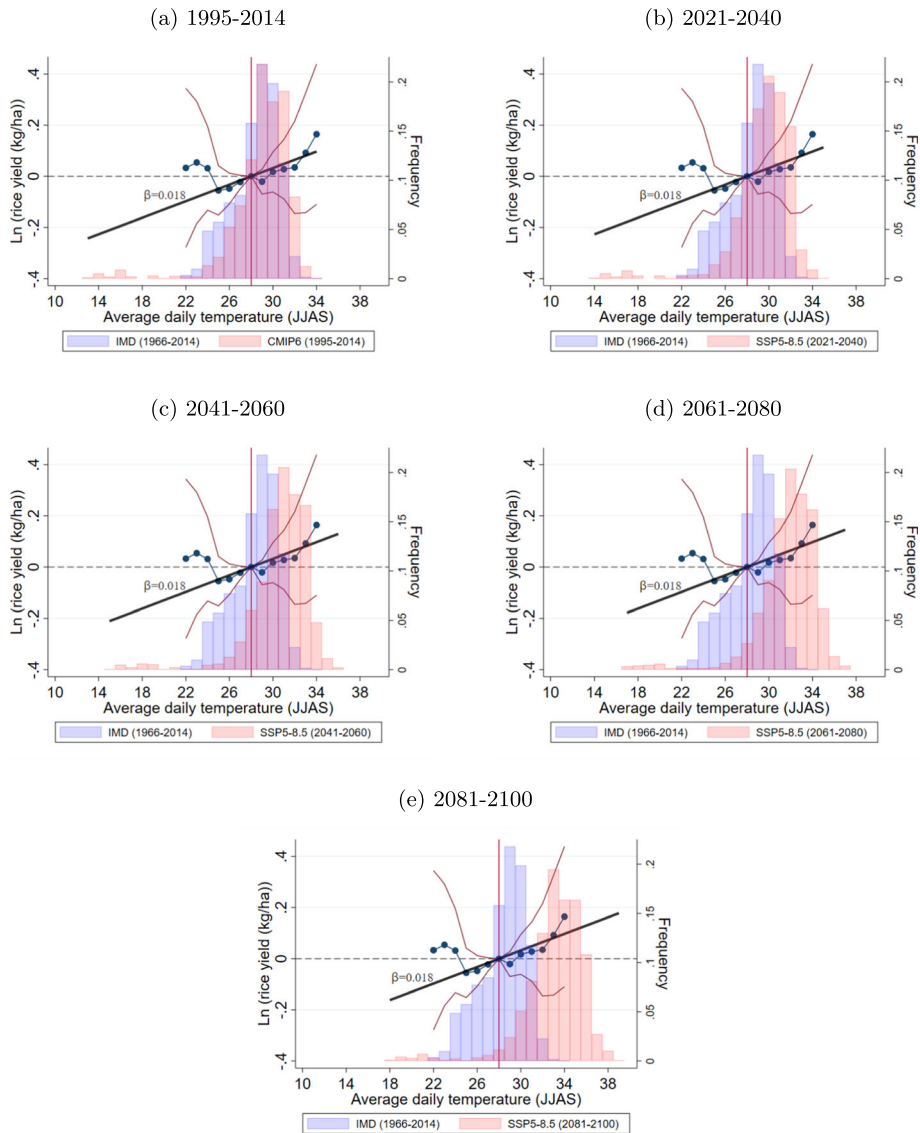


Fig. 18 Estimation results for rice and projected average temperature (JJAS) distributions (SSP5-8.5). The plotted coefficients refer to the coefficients $\hat{\beta}$ as estimated according to Eq. 1. Red lines indicate the respective 95% confidence interval. The vertical red line refers to the omitted bin, which corresponds to the sample mean. All Panels display the results for average daily temperature for the months of June, July, August and September (JJAS) on rice yield. Standard errors are clustered at the state level. The regression further includes district and year fixed effects, which are not reported. The blue colored bars display the binned distribution of the respective variables based on the the years 1966-2014. Panel (a) depicts the projected temperature (JJAS) distribution for the reference period. Panel (b) - (e) depict the projections for the future periods under under SSP5-8.5. Data sources: ICRISAT, IMD, CMIP6

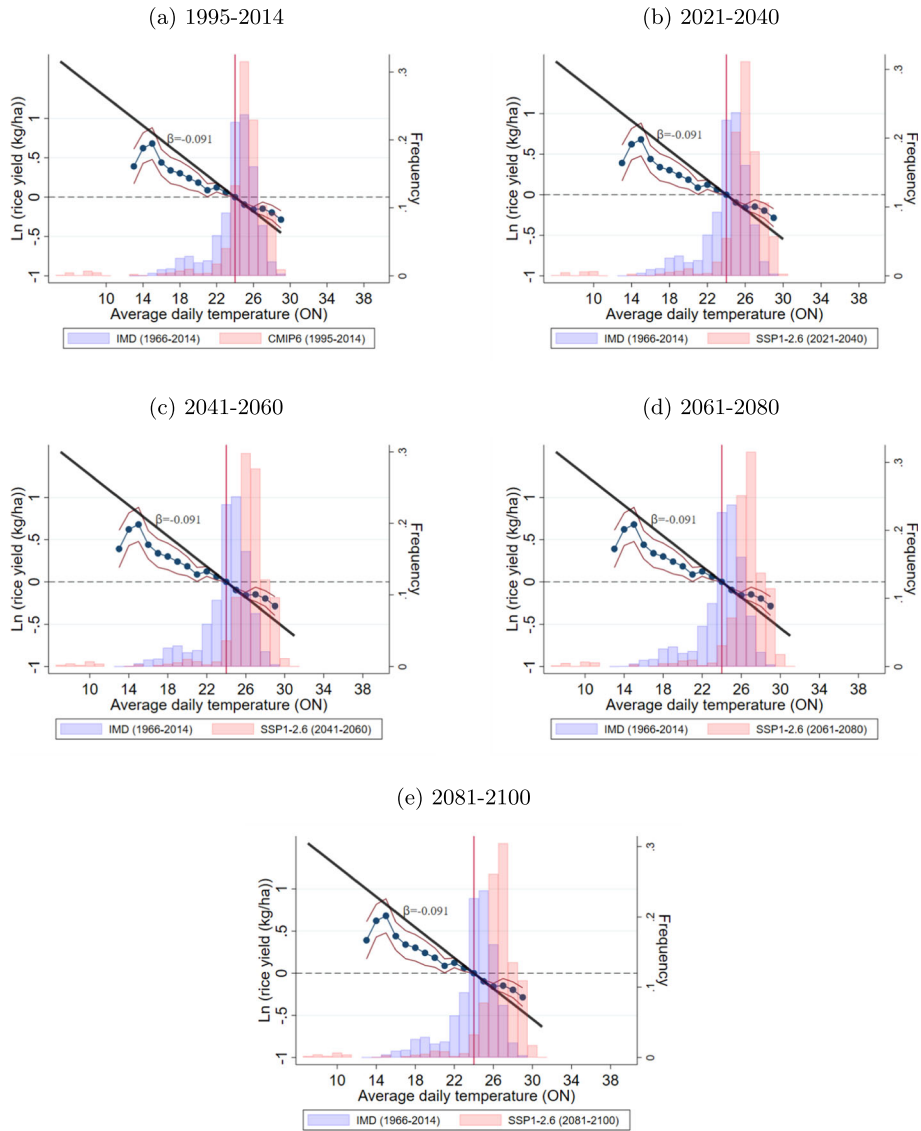


Fig. 19 Estimation results for rice and projected average temperature (ON) distributions (SSP1-2.6). The plotted coefficients refer to the coefficients $\hat{\beta}$ as estimated according to Eq. 1. Red lines indicate the respective 95% confidence interval. The vertical red line refers to the omitted bin, which corresponds to the sample mean. All Panels display the results for average daily temperature for the months of October and November (ON) on rice yield. Standard errors are clustered at the state level. The regression further includes district and year fixed effects, which are not reported. The blue colored bars display the binned distribution of the respective variables based on the the years 1966-2014. Panel (a) depicts the projected temperature (ON) distribution for the reference period. Panel (b) - (e) depict the projections for the future periods under under SSP1-2.6. Data sources: ICRISAT, IMD, CMIP6

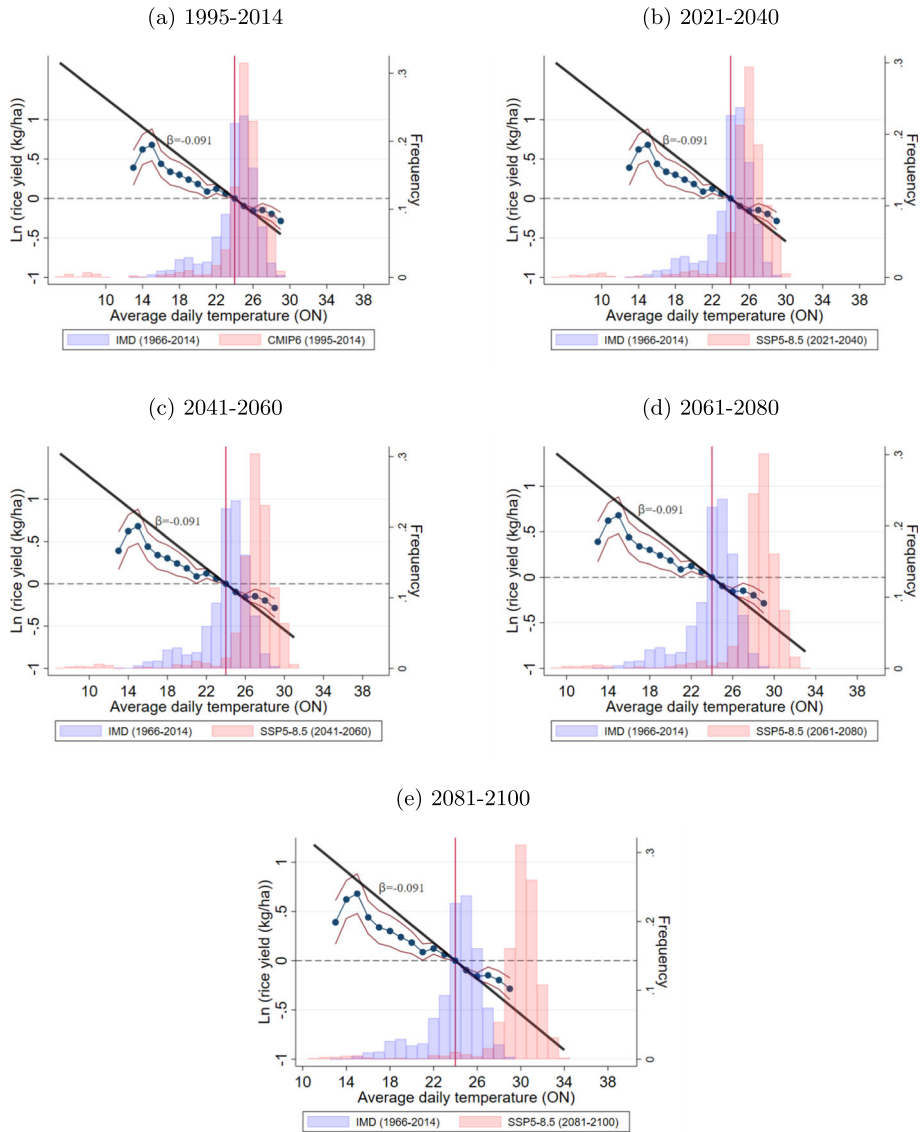


Fig. 20 Estimation results for rice and projected average temperature (ON) distributions (SSP5-8.5). The plotted coefficients refer to the coefficients $\hat{\beta}$ as estimated according to Eq. 1. Red lines indicate the respective 95% confidence interval. The vertical red line refers to the omitted bin, which corresponds to the sample mean. All Panels display the results for average daily temperature for the months of October and November (ON) on rice yield. Standard errors are clustered at the state level. The regression further includes district and year fixed effects, which are not reported. The blue colored bars display the binned distribution of the respective variables based on the the years 1966-2014. Panel (a) depicts the projected temperature (ON) distribution for the reference period. Panel (b) - (e) depict the projections for the future periods under under SSP5-8.5. Data sources: ICRISAT, IMD, CMIP6

Prediction Results

This section complements Section “Climate Change Projections” in the main paper. Figure 21 plots the absolute changes in predicted rice yield. Figure 22 and 23 plot the model specific predictions in rice yield changes for the long-term. Figures 24, 25, 26, 27, 28, 29 and 30 show the results for changes in predicted yield, averaged across all 8 models, for all other crops than rice. Figure 31 plots the annual moving average of predicted rice yield relative to the reference period.

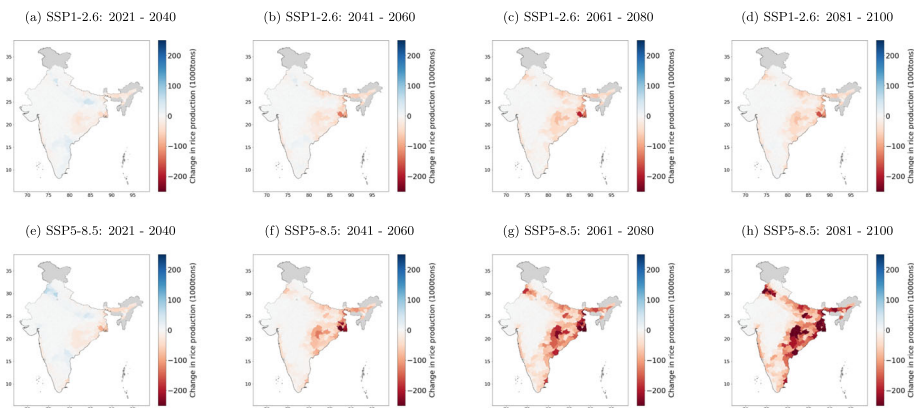


Fig. 21 Predicted rice production changes (evaluated at total production 1995 - 2014). Figure 21 shows the predicted changes in total rice production evaluated at the average district rice production (in 1000t) during the reference period (1995-2014). Panel (a) - (d) display the predicted change in rice production under SSP1-2.6 for the future periods relative to the reference period 1995-2014. Panel (e) - (f) show the predicted change in rice production under SSP5-8.5. All predictions correspond to the average of the predictions of all 8 selected climate models. Data sources: ICRISAT, IMD, CMIP6

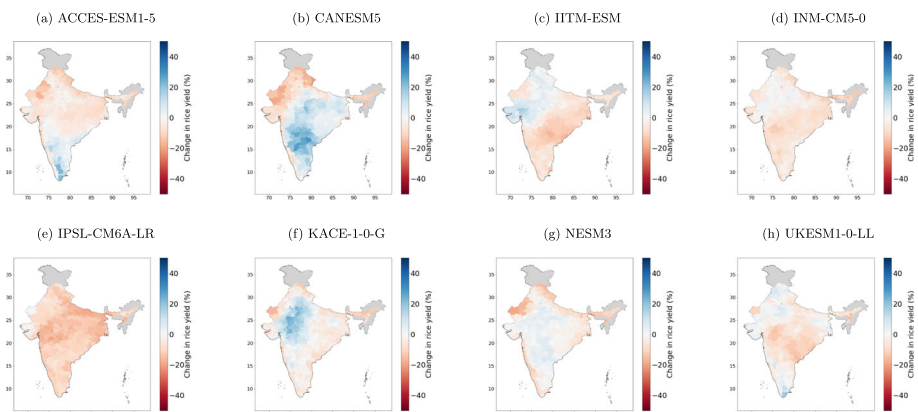


Fig. 22 SSP1-2.6: Predicted rice yield changes (2081 - 2100). Figure 22 shows the predicted changes in rice yield (\hat{Y}) based on Eq. 3 for each climate model separately in the long-term (2081-2100). Panel (a) displays the predicted change in rice yield under SSP1-2.6 as projected by the ACCES-ESM1-5 model. Panel (b) - (h) show the predicted changes in rice yield under SSP1-2.6 as projected by the remaining models. All predictions correspond to the average of the predictions of all 8 selected climate models. Data sources: ICRISAT, IMD, CMIP6

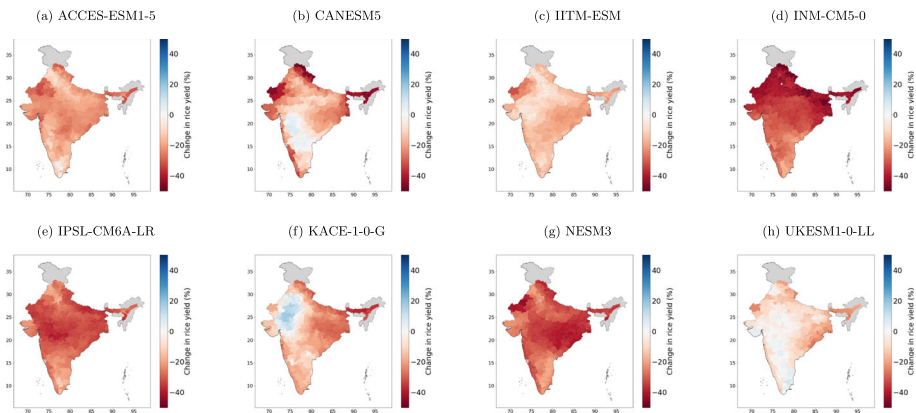


Fig. 23 SSP5-8.5: Predicted rice yield changes (2081 - 2100). Figure 23 shows the predicted changes in rice yield (\hat{Y}) based on Eq. 3 for each climate model separately in the long-term (2081–2100). Panel (a) displays the predicted change in rice yield under SSP5-8.5 as projected by the ACCES-ESM1-5 model. Panel (b) - (h) show the predicted changes in rice yield under SSP5-8.5 as projected by the remaining models. All predictions correspond to the average of the predictions of all 8 selected climate models. Data sources: ICRIASAT, IMD, CMIP6

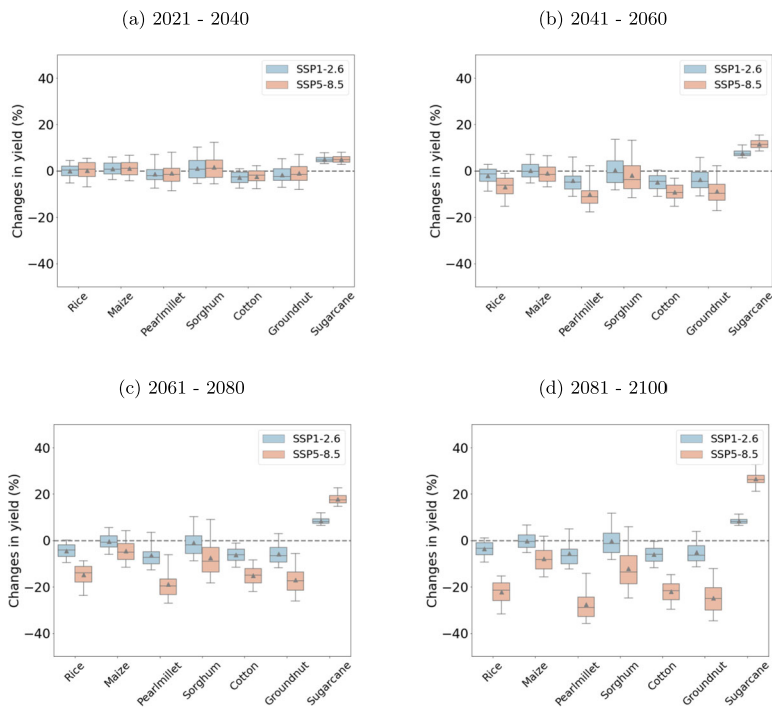


Fig. 24 Comparison across crops. Figure 24 shows the distribution of the predicted changes in yield (\hat{Y}) as predicted based on Eq. 3 across India for each crop separately. Panel (a) depicts the results for the period of 2021–2040 compared to the reference period of 1995–2014, where blue boxplots display the results under SSP1-2.6 and red boxplots under SSP5-8.5. Triangles refer to the mean and the solid lines within the boxplots to the median. Panel (b) - (d) depict the results for the remaining periods. Data sources: ICRIASAT, IMD, CMIP6

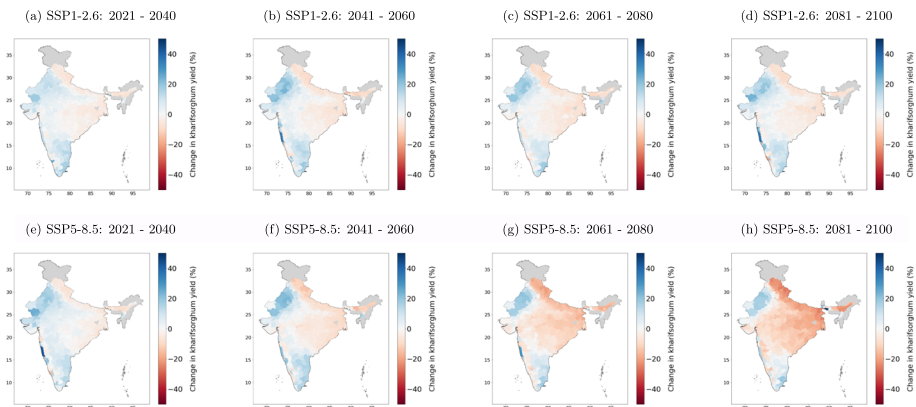


Fig. 25 Predicted sorghum yield changes. Figure 25 shows the predicted changes in sorghum yield (\hat{Y}) based on Eq. 3. Panel (a) - (d) display the predicted change in sorghum yield under SSP1-2.6 for the future periods relative to the reference period 1995-2014. Panel (e) - (f) show the predicted change in sorghum yield under SSP5-8.5. All predictions correspond to the average of the predictions of all 8 selected climate models. Data sources: ICRISAT, IMD, CMIP6

Figure 24 shows the average predicted changes across crops by global warming scenario relative to the period of 1995-2014. In the short run there is no significant difference for all crops between the two SSPs. Again the differences become more pronounced in the long-term, with all crops decreasing except sugarcane. In the long run sugarcane yield is predicted to increase on average by 8.2% (SSP1-2.6) or 25.6% (SSP5-8.5) respectively. Sorghum yield is predicted to increase on average by 0.9% (SSP1-2.6) and decrease by 8.8% (SSP5-

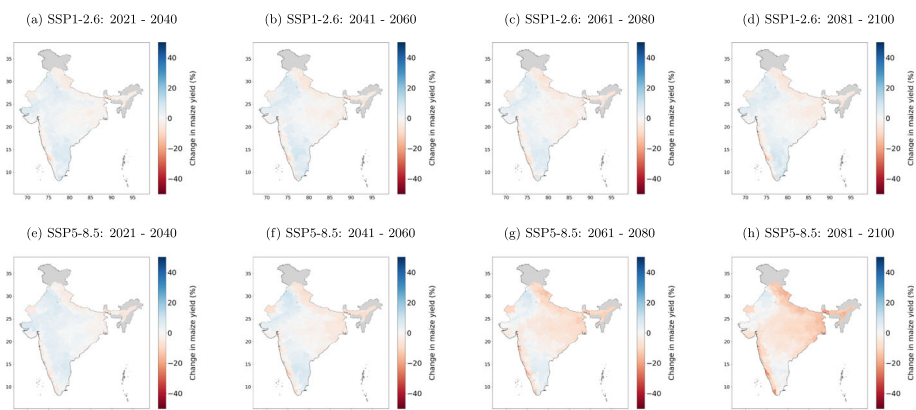


Fig. 26 Predicted maize yield changes. Figure 26 shows the predicted changes in maize yield (\hat{Y}) based on Eq. 3. Panel (a) - (d) display the predicted change in maize yield under SSP1-2.6 for the future periods relative to the reference period 1995-2014. Panel (e) - (f) show the predicted change in maize yield under SSP5-8.5. All predictions correspond to the average of the predictions of all 8 selected climate models. Data sources: ICRISAT, IMD, CMIP6

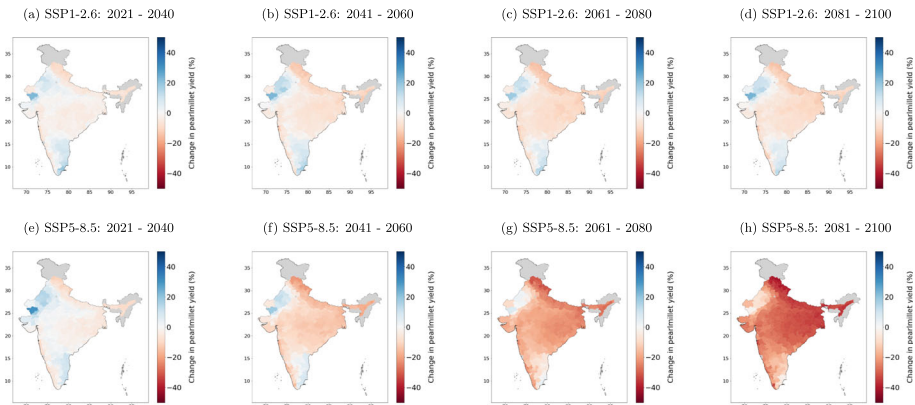


Fig. 27 Predicted pearl millet yield changes. Figure 27 shows the predicted changes in pearl millet yield (\hat{Y}) based on Eq. 3. Panel (a) - (d) display the predicted change in pearl millet yield under SSP1-2.6 for the future periods relative to the reference period 1995-2014. Panel (e) - (f) show the predicted change in pearl millet yield under SSP5-8.5. All predictions correspond to the average of the predictions of all 8 selected climate models. Data sources: ICRISAT, IMD, CMIP6

8.5). Pearlmillet provides the biggest difference between the SSPs in the long-term, with a predicted decrease in yield of on average 5.4% under the SSP1-2.6 scenario and 27.7% under the SSP5-8.5 scenario.

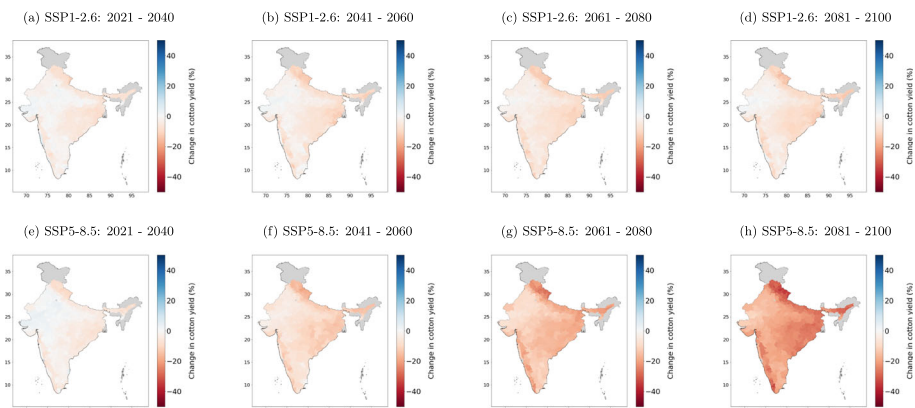


Fig. 28 Predicted cotton yield changes. Figure 28 shows the predicted changes in cotton yield (\hat{Y}) based on Eq. 3. Panel (a) - (d) display the predicted change in cotton yield under SSP1-2.6 for the future periods relative to the reference period 1995-2014. Panel (e) - (f) show the predicted change in cotton yield under SSP5-8.5. All predictions correspond to the average of the predictions of all 8 selected climate models. Data sources: ICRISAT, IMD, CMIP6

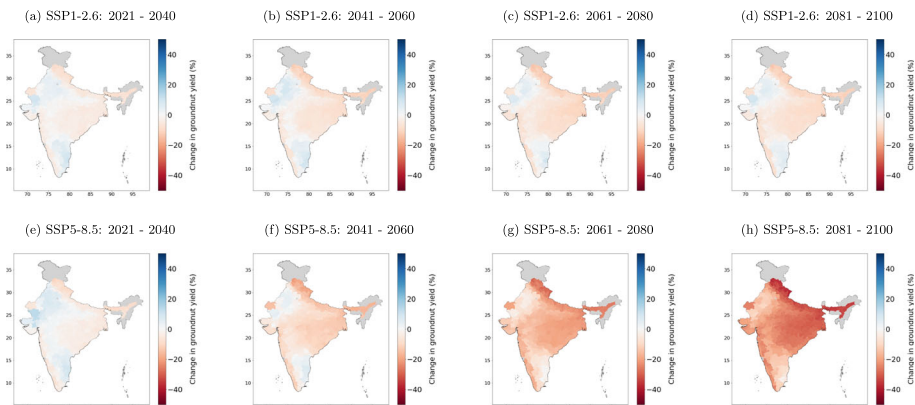


Fig. 29 Predicted groundnut yield changes. Figure 29 shows the predicted changes in groundnut yield (\hat{Y}) based on Eq. 3. Panel (a) – (d) display the predicted change in groundnut yield under SSP1-2.6 for the future periods relative to the reference period 1995–2014. Panel (e) – (f) show the predicted change in groundnut yield under SSP5-8.5. All predictions correspond to the average of the predictions of all 8 selected climate models. Data sources: ICRISAT, IMD, CMIP6

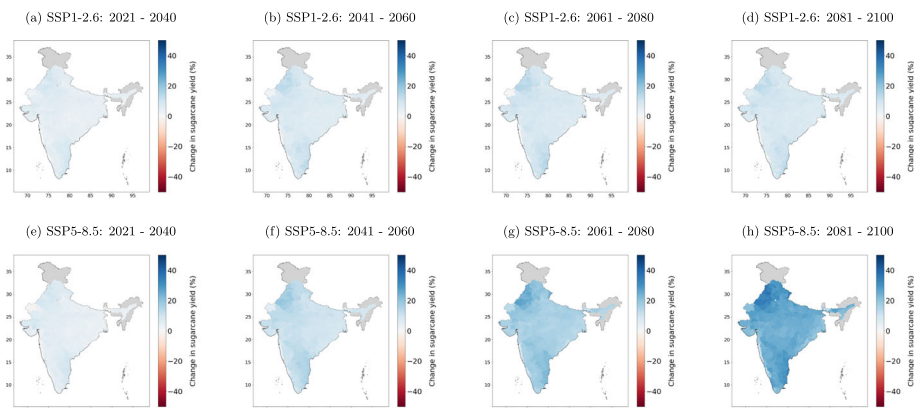


Fig. 30 Predicted sugarcane yield changes. Figure 30 shows the predicted changes in sugarcane yield (\hat{Y}) based on Eq. 3. Panel (a) – (d) display the predicted change in sugarcane yield under SSP1-2.6 for the future periods relative to the reference period 1995–2014. Panel (e) – (f) show the predicted change in sugarcane yield under SSP5-8.5. All predictions correspond to the average of the predictions of all 8 selected climate models. Data sources: ICRISAT, IMD, CMIP6

Decomposition of Climate Change Impacts

This section complements Section “[Decomposition of Climate Change Impacts](#)” in the main paper. Figures 32, 33 and 34 show the prediction results for ceteris paribus changes in the projections of the different weather variables.

Sensitivity of Results

The following section provides an explanation of the convexity of the slope of Fig. 6, which illustrates the sensitivity of the relative changes in rice yield predictions with respect to temperature in ON. In the initial prediction results, we compare the predicted rice yield of a future

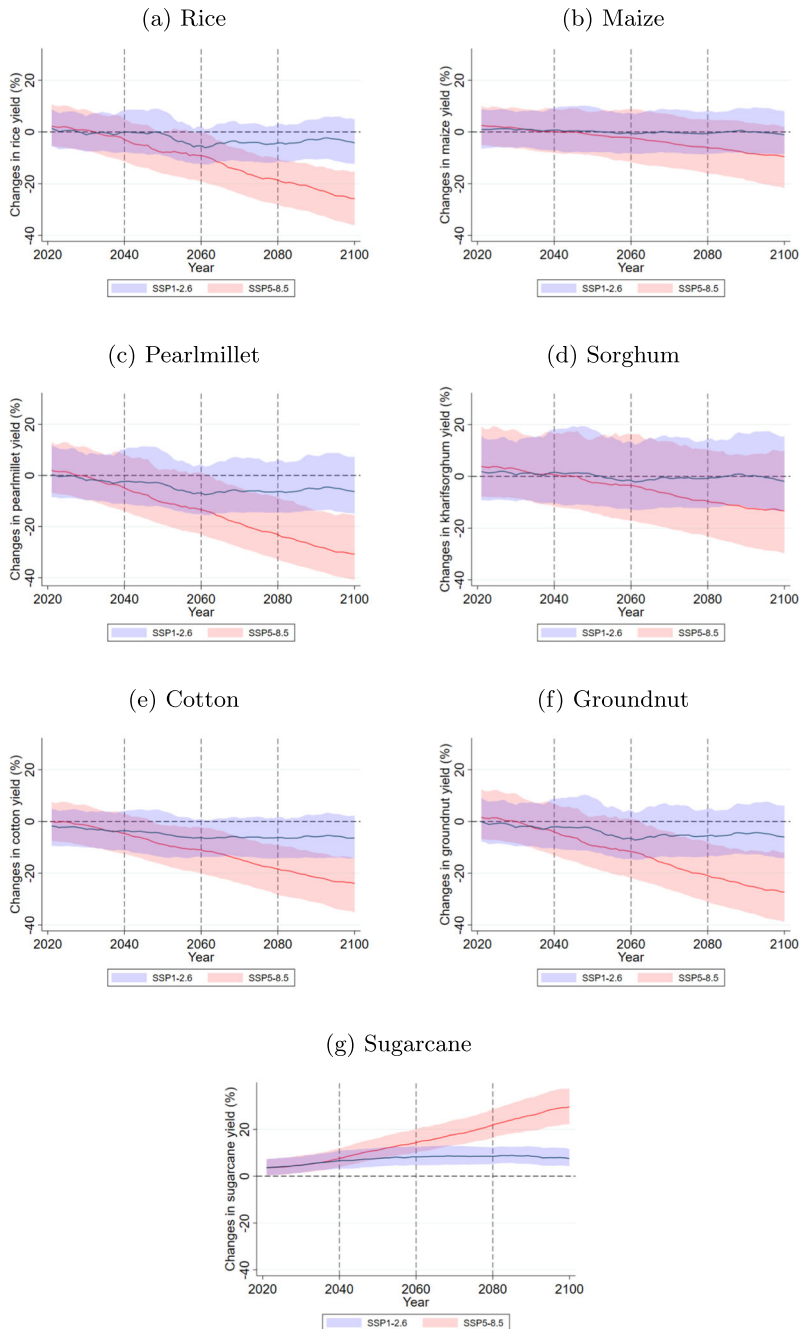


Fig. 31 Moving averages by SSP. Figure 31 shows the moving averages with 5 leads and lags in predicted rice yield ($\hat{y}_{it sm}$) based on Eq. 2 averaged across all 8 climate models and relative to the predicted mean rice yield of the reference period (1995–2014). The blue-shaded and red-shaded area display the 95% range of of the district prediction under SSP1-2.6 and SSP5-8.5 respectively. The lines refer to the annual average across all districts in India. Data sources: CMIP6 and author's estimated coefficients based on ICRISAT and IMD

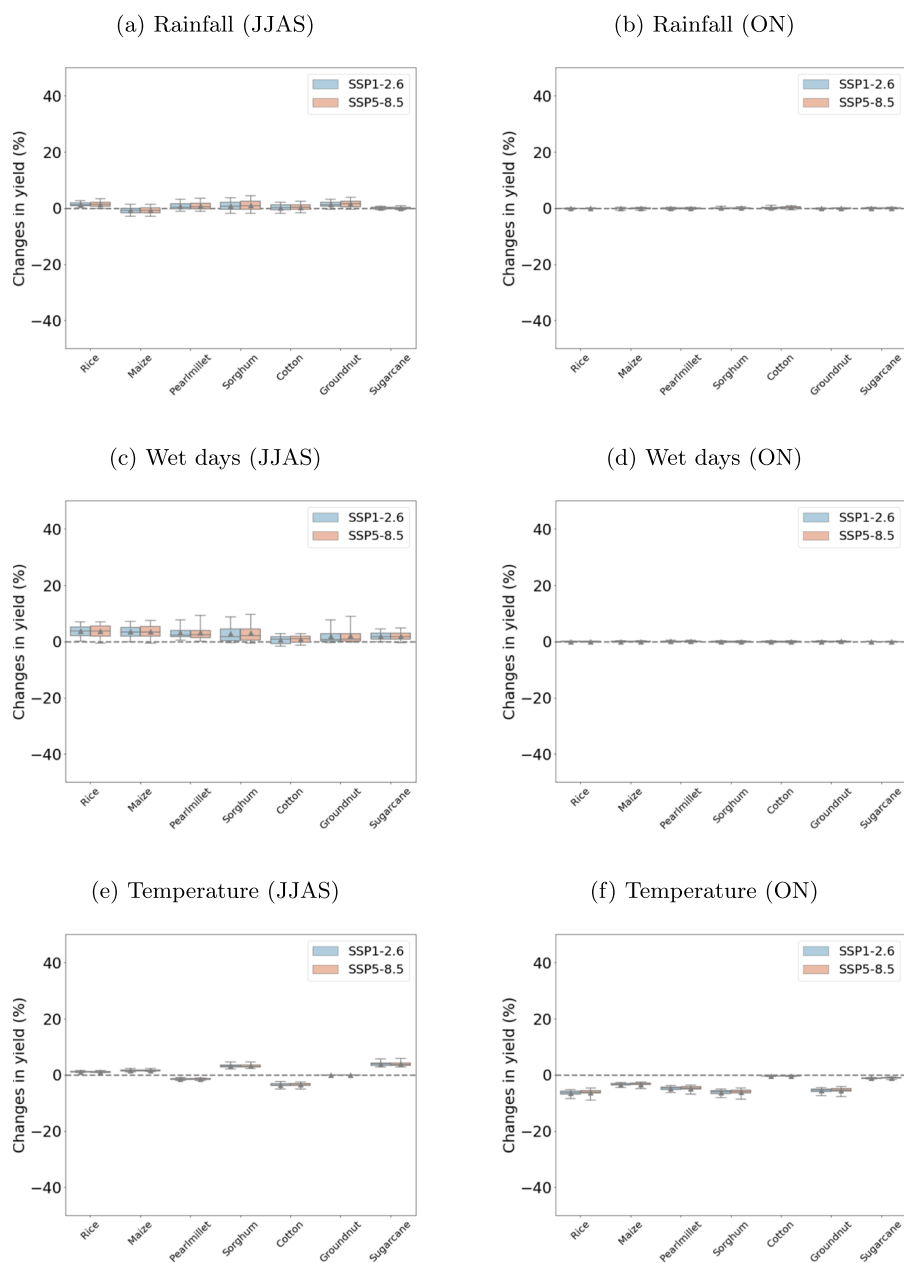


Fig. 32 Estimation results by variable (2021-2040). Figure 32 shows distribution of the predicted changes in yield (\hat{Y}) as predicted based on Eq. 3 across India for all crops and each variable separately. Panel(a) depicts the results for the period of 2021-2040 compared to the reference period of 1995-2014, when keeping all variables at the level of the reference period except rainfall (JJAS). Panel (b) - (d) depict the results for the remaining variables. Blue boxplots display the results under SSP1-2,6 and red boxplots under SSP5-8.5. Triangles refer to the mean and the solid lines within the boxplots to the median. Data sources: ICRISAT, IMD, CMIP6

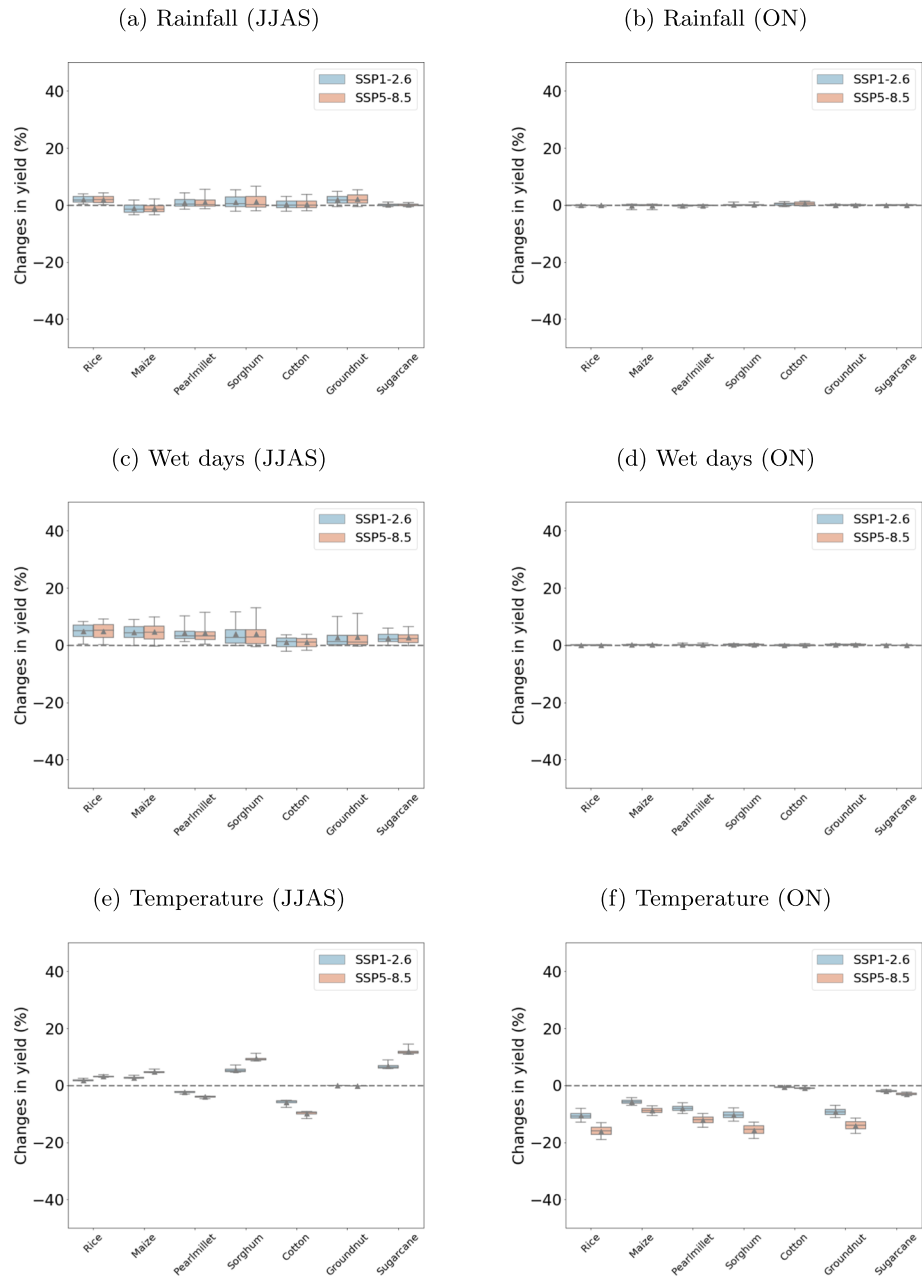


Fig. 33 Estimation results by variable (2041–2060). Figure 33 shows distribution of the predicted changes in yield (\hat{Y}) as predicted based on Eq. 3 across India for all crops and each variable separately. Panel(a) depicts the results for the period of 2041–2060 compared to the reference period of 1995–2014, when keeping all variables at the level of the reference period except rainfall (JJAS). Panel (b) - (d) depict the results for the remaining variables. Blue boxplots display the results under SSP1-2,6 and red boxplots under SSP5-8.5. Triangles refer to the mean and the solid lines within the boxplots to the median. Data sources: ICRISAT, IMD, CMIP6

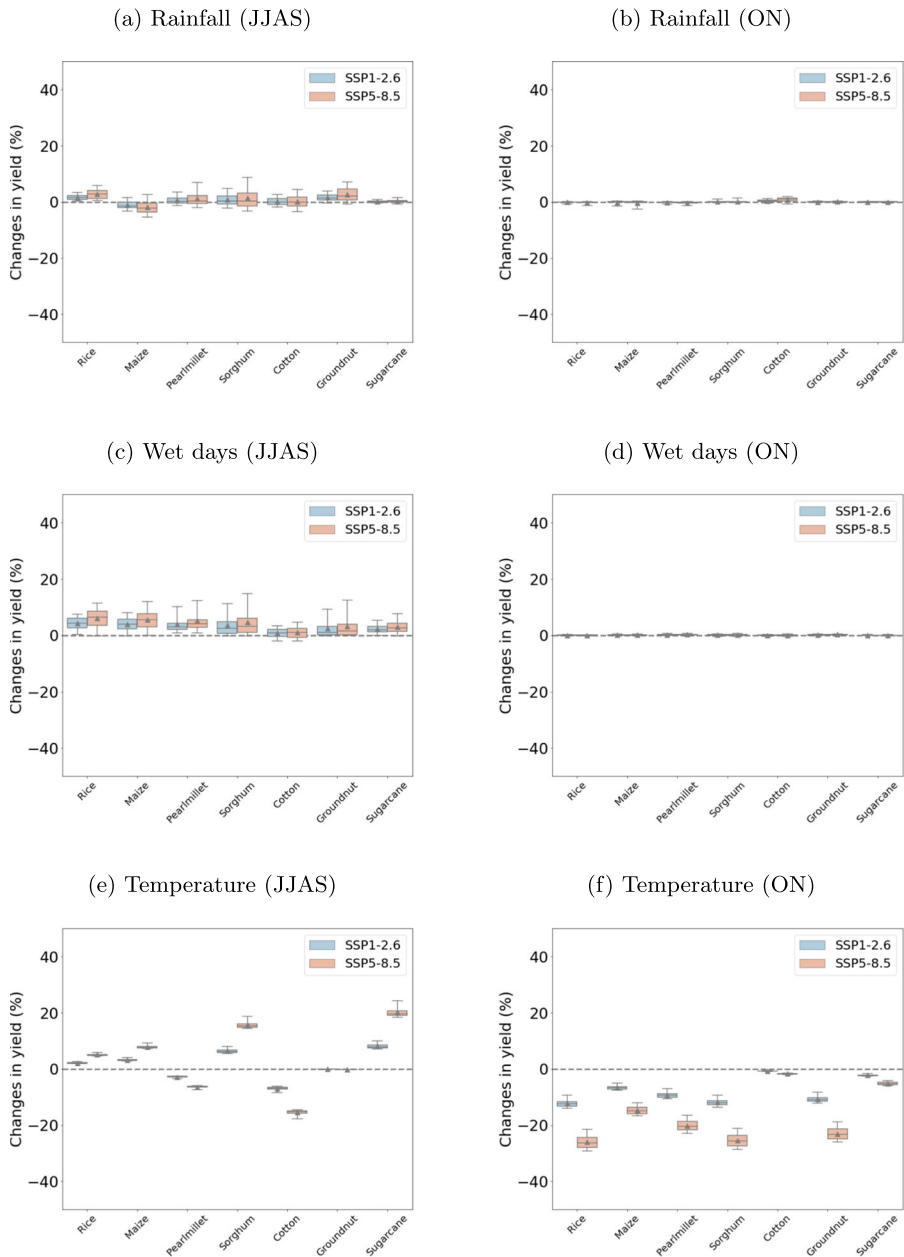


Fig. 34 Estimation results by variable (2061-2080). Figure 34 shows distribution of the predicted changes in yield (\hat{Y}) as predicted based on Eq. 3 across India for all crops and each variable separately. Panel(a) depicts the results for the period of 2061-2080 compared to the reference period of 1995-2014, when keeping all variables at the level of the reference period except rainfall (JJAS). Panel (b) - (d) depict the results for the remaining variables. Blue boxplots display the results under SSP1-2,6 and red boxplots under SSP5-8.5. Triangles refer to the mean and the solid lines within the boxplots to the median. Data sources: ICRISAT, IMD, CMIP6

period with the reference period (see Eq. 3 for details). For reasons of simplicity, we assume two periods, where period 1 refers to the reference period and period 2 to the future period. Equation 5 shows for the reference period, how the log of the predicted rice yield ($\ln(\hat{y}_1)$) can be split in two parts. The first part covers all other variables apart from temperature in ON and their coefficients such as rainfall, number of wet days and temperature in JJAS ($RAIN_1$). The second part represents the predicted impact of temperature in ON, which depends on the estimated coefficient (β) and the projected temperature itself ($TEMP_1$). Next, we can transform the log of the predicted yield into the actual predicted rice yield (\hat{y}_1).

$$\begin{aligned}\ln(\hat{y}_1) &= RAIN_1 + \beta \times TEMP_1 \\ \Leftrightarrow \hat{y}_1 &= e^{RAIN_1 + \beta \times TEMP_1}\end{aligned}\quad (5)$$

Equation 6 denotes the same procedure for the future period.

$$\begin{aligned}\ln(\hat{y}_2) &= RAIN_2 + \beta \times TEMP_2 \\ \Leftrightarrow \hat{y}_2 &= e^{RAIN_2 + \beta \times TEMP_2}\end{aligned}\quad (6)$$

The relative changes in predicted rice yield between the reference period and the future period can be written and simplified as follows:

$$\hat{Y} = \frac{\hat{y}_2 - \hat{y}_1}{\hat{y}_1} = \frac{e^{RAIN_2 + \beta \times TEMP_2} - e^{RAIN_1 + \beta \times TEMP_1}}{e^{RAIN_1 + \beta \times TEMP_1}} \quad (7)$$

$$= \frac{e^{RAIN_2 + \beta \times TEMP_2}}{e^{RAIN_1 + \beta \times TEMP_1}} - 1 \quad (8)$$

$$= e^{RAIN_2 + \beta \times TEMP_2 - (RAIN_1 + \beta \times TEMP_1)} - 1 \quad (9)$$

$$= e^{(RAIN_2 - RAIN_1) + \beta \times (TEMP_2 - TEMP_1)} - 1 \quad (10)$$

In a next step, we differentiate Eq. 10 with respect to β , which denotes the estimated temperature effect in ON. This yields Eq. 11.

$$\hat{Y}'(\beta) = (TEMP_2 - TEMP_1) \times e^{(RAIN_2 - RAIN_1) + (TEMP_2 - TEMP_1) \times \beta} \quad (11)$$

It is evident, that the slope is steeper the larger the difference between $TEMP_2$ and $TEMP_1$. In order to check if the function is convex or concave, we take the second derivative, where $Y''(\beta) > 0$ would imply convexity. The second derivative is given by Eq. 12.

$$\hat{Y}''(\beta) = \underbrace{(TEMP_2 - TEMP_1)^2}_{>0, \text{ if } TEMP_2 \neq TEMP_1} \times \underbrace{e^{(RAIN_2 - RAIN_1) + (TEMP_2 - TEMP_1) \times \beta}}_{>0} \quad (12)$$

$>0, \text{ if } TEMP_2 \neq TEMP_1$

The results show indeed that $Y''(\beta) > 0$ as long as $TEMP_2 \neq TEMP_1$. Hence, the sensitivity of the relative changes in rice yield predictions with respect to temperature in ON is convex for both global warming scenarios (SSP1-2.6 and SSP5-8.5). However, due to the smaller future increase in temperature in the sustainable scenario (blue-shaded area in Fig. 6), the convexity is less pronounced than in the worst case scenario (red-shaded area). This also explains, why the plot in the worst case scenario becomes more convex over time, since the projected future temperature in ON becomes higher on average over time.

Acknowledgements We thank Anders Levermann for his valuable feedback throughout the process. We also thank Thomas Bauer for helpful comments and suggestions. Furthermore, we are grateful for valuable remarks from seminar and conference participants at the RTG 2484 "Regional Disparities and Economic Policy", the Leibniz Environment and Development Symposium (LEADS) 2022, the VfS Junior Environmental Economics Workshop 2022 and the 17th Annual EfD meeting 2023. Besides, we thank Stefan Lange for bias correcting the data of 11 additional CMIP6 models. We also acknowledge the World Climate Research Programme's Working Group on Coupled Modelling, which is responsible for CMIP, and we thank the climate modeling groups for producing and making available their model output. The research was partially financially supported by the German Research Foundation (DFG) and the Heinrich-Boell Foundation who did not have any influence on the study design; in the collection, analysis and interpretation of data; in the writing of the report; and in the decision to submit the article for publication. The authors gratefully acknowledge financial support by the Deutsche Gesellschaft für Internationale Zusammenarbeit (GIZ) GmbH on behalf of the Government of the Federal Republic of Germany and Federal Ministry for Economic Cooperation and Development (BMZ).

Author Contributions All authors contributed to the study conception and design. A.K. processed and provided the climate model projections. J.G. combined all data sets and performed the econometric analysis. All authors discussed the results and provided critical feedback. All authors wrote the paper.

Data Availability All data sources used in the paper are publicly available. The combined data set will be made publicly available after publication. ICRIAT District Level Database: <http://data.icrisat.org/dld/> Gridded maximum temperature data: https://www.imdpune.gov.in/cmpg/Griddata/Max_1_Bin.html Gridded minimum temperature data: https://www.imdpune.gov.in/cmpg/Griddata/Min_1_Bin.html Gridded rainfall data: https://www.imdpune.gov.in/cmpg/Griddata/Rainfall_25_Bin.html Climate model projections (CMIP6) data: <https://esgf-data.dkrz.de/search/cmip6-dkrz/>

Declarations

Competing interests The authors declare no competing interests.

Open Access This article is licensed under a Creative Commons Attribution 4.0 International License, which permits use, sharing, adaptation, distribution and reproduction in any medium or format, as long as you give appropriate credit to the original author(s) and the source, provide a link to the Creative Commons licence, and indicate if changes were made. The images or other third party material in this article are included in the article's Creative Commons licence, unless indicated otherwise in a credit line to the material. If material is not included in the article's Creative Commons licence and your intended use is not permitted by statutory regulation or exceeds the permitted use, you will need to obtain permission directly from the copyright holder. To view a copy of this licence, visit <http://creativecommons.org/licenses/by/4.0/>.

References

- Adler RF et al (2003) The version-2 global precipitation climatology project (GPCP) monthly precipitation analysis (1979-present). *J Hydrometeorol* 4(6):1147–1167
- Allen T, Atkin D (2022) Volatility and the Gains from Trade. *Econometrica* 90(5):2053–2092
- Aragón FM, Oteiza F, Rud JP (2021) Climate change and agriculture: Subsistence farmers' response to extreme heat. *Am Econ J Econ Policy* 13(1):1–35
- Auffhammer M et al (2012) Climate change, the monsoon, and rice yield in India. *Climatic Change*, 111(2):411–424, 3
- Auffhammer M et al (2020) Using weather data and climate model output in economic analyses of climate change. *Rev Environ Econ Policy* 7(2):181–198
- Burke M, Emerick K (2016) Adaptation to climate change: Evidence from us agriculture. *Rev Environ Econ Policy* 8(3):106–40
- Carleton TA (2017) Crop-damaging temperatures increase suicide rates in India. *Proceedings of the national academy of sciences* 114(33):8746–8751
- Chaturvedi RK et al (2012) Multi-model climate change projections for India under representative concentration pathways. *Curr Sci* 103(7):791–802

- Chen S, Chen X, Xu J (2016) Impacts of climate change on agriculture: Evidence from china. *J Environ Econ Manag* 76:105–124
- Chuang Y (2019) Climate variability, rainfall shocks, and farmers' income diversification in India. *Econ Lett* 174:55–61
- Colmer J (2021) Temperature, labor reallocation, and industrial production: Evidence from India. *Am Econ J Appl Econ* 13(4):101–24
- Cucchi M et al (2020) WFDE5: bias-adjusted ERA5 reanalysis data for impact studies. *Earth Syst Sci Data* 12(3):2097–2120
- Dell M et al (2012) Temperature shocks and economic growth: Evidence from the last half century. *American Econ J Macroecon* 4(3):66–95
- Dell M et al (2014) What Do We Learn from the Weather? The New Climate-Economy Literature. *J Econ Litt* 52(3):740–98, 9
- Deschênes O, Greenstone M (2011) Climate change, mortality, and adaptation: Evidence from annual fluctuations in weather in the us. *American Econ J Appl Econ* 3(4):152–85
- FAO Faostat (2022) data retrieved from FAOSTAT. <https://www.fao.org/faostat/en/#home>
- Fishman R (2016) More uneven distributions overturn benefits of higher precipitation for crop yields. *Environ Res Lett* 11(2):024004, 2
- Frieler K, Schaubberger B, Arneth A, Balkovič J, Chrysanthacopoulos J, Deryng D, Elliott J, Folberth C, Khabarov N, Müller C et al (2017) Understanding the weather signal in national crop-yield variability. *Earth's future* 5(6):605–616
- Ha K-J et al (2020) Future changes of summer monsoon characteristics and evaporative demand over Asia in CMIP6 simulations *Geophysical Research Letters*, 47(8):e2020GL087492
- Hersbach H et al (2020) The ERA5 global reanalysis. *Q J R Meteorol Soc* 146(730):1999–2049
- Hsiang S (2016) Climate econometrics. *Ann Rev Resour Econ* 8:43–75
- IPCC (2022) Climate Change 2022: Impacts, Adaptation, and Vulnerability. Contribution of Working Group II to the Sixth Assessment Report of the Intergovernmental Panel on Climate Change. Cambridge University Press
- Jayachandran S (2006) Selling labor low: Wage responses to productivity shocks in developing countries. *J Polit Econ* 114(3):538–575
- Katzenberger A, Levermann A, Schewe J, Pongratz J (2022) Intensification of very wet monsoon seasons in India under global warming. *Geophys Res Lett* 59:e2022GL098856
- Katzenberger A, Schewe J, Pongratz J, Levermann A (2021) Robust increase of Indian monsoon rainfall and its variability under future warming in CMIP6 models. *Earth Syst Dynamics* 12(2):367–386, 4
- Kumar KK et al (2004) Climate impacts on Indian agriculture. *Int J Climatol* 24(11):1375–1393, 9
- Krishnan R et al (2020) Assessment of Climate Change over the Indian Region: A Report of the Ministry of Earth Sciences (MoES). Government of India, Springer Nature
- Kumar V et al (2010) Analysis of long-term rainfall trends in India. *Hydrological Sciences Journal-Journal des Sciences Hydrologiques* 55(4):484–496
- Lange S (2019) Trend-preserving bias adjustment and statistical downscaling with ISIMIP3BASD (v1.0). *Geosci Model Dev* 12(7):3055–3070
- Lange S (2019) WFDE5 over land merged with ERA5 over the ocean (W5E5). V. 1.0. GFZ Data Services
- Li T et al (2015) Uncertainties in predicting rice yield by current crop models under a wide range of climatic conditions. *Glob Chang Biol* 21(3):1328–1341
- Meher JK et al (2015) Recent trends in monsoon rainfall and its effect on yield of kharif rice in five subdivisions of North India. *J Agroecol Nat Resour Manage* 2(3):192–196
- Menon A, Levermann A, Schewe J, Lehmann J, Frieler K (2013) Consistent increase in Indian monsoon rainfall and its variability across CMIP-5 models. *Earth Syst Dyn* 4:287–300
- Minoli S et al (2022) Global crop yields can be lifted by timely adaptation of growing periods to climate change. *Nat Commun* 13(1):1–10
- Müller C, Robertson RD (2014) Projecting future crop productivity for global economic modeling. *Agric Econ* 45(1):37–50
- O'Neill BC et al (2017) The roads ahead: Narratives for shared socioeconomic pathways describing world futures in the 21st century. *Glob Environ Chang* 42:169–180
- Pai DS et al (2014) Development of a new high spatial resolution (0.25° × 0.25°) Long Period (1901–2010) daily gridded rainfall data set over India and its comparison with existing data sets over the region. *Mausam*, pp 1–18
- Palagi E et al (2022) Climate change and the nonlinear impact of precipitation anomalies on income inequality. *Proceedings of the national academy of sciences* 119(43):e2203595119
- Panda A et al (2019) Impact of climate variability on crop yield in Kalahandi, Bolangir, and Koraput districts of Odisha, India. *Climate* 7(11):126

- Prasanna V (2014) Impact of monsoon rainfall on the total foodgrain yield over India. *J Earth Syst Sci* 123(5):1129–1145
- Preethi B et al (2019) Variability of Indian summer monsoon droughts in CMIP5 climate models. *Clim Dyn* 53(3):1937–1962
- Revadekar JV, Preethi B (2012) Statistical analysis of the relationship between summer monsoon precipitation extremes and foodgrain yield over India. *Int J Climatol* 32(3):419–429
- Rosenzweig C et al (2014) Assessing agricultural risks of climate change in the 21st century in a global gridded crop model intercomparison. *Proceedings of the national academy of sciences* 111(9):3268–3273
- Rosenzweig MR, Binswanger HP (1992) Wealth, weather risk, and the composition and profitability of agricultural investments, vol 1055. World Bank Publications
- Schlenker W, Roberts MJ (2009) Nonlinear temperature effects indicate severe damages to us crop yields under climate change. *Proceedings of the national academy of sciences* 106(37):15594–15598
- Seth A et al (2019) Monsoon responses to climate changes—connecting past, present and future. *Curr Clim Chang Rep* 5(2):63–79
- Singh K et al (2017) Mapping regional risks from climate change for rainfed rice cultivation in India. *Agric Syst* 156(76–84):9
- Soora NK et al (2013) An assessment of regional vulnerability of rice to climate change in India. *Clim Chang* 118(3–4):683–699, 6
- Srivastava AK et al (2009) Development of a high resolution daily gridded temperature data set (1969–2005) for the Indian region. *Atmos Sci Lett* 10:249–254
- Taraz V (2017) Adaptation to climate change: Historical evidence from the indian monsoon. *Environ Dev Econ* 22(5):517–545
- Taraz V (2018) Can farmers adapt to higher temperatures? Evidence from India. *World Development* 112:205–219
- Van Vuuren DP et al (2014) A new scenario framework for climate change research: scenario matrix architecture. *Clim Chang* 122(3):373–386
- Vogel E et al (2019) The effects of climate extremes on global agricultural yields. *Environ Res Lett* 14(5):054010
- Webster PJ et al (1998) Monsoons: Processes, predictability, and the prospects for prediction. *J Geophys Res Oceans* 103(C7):14451–14510
- Weedon GP et al (2010) The WATCH Forcing Data 1958–2001: A meteorological forcing dataset for land surface- and hydrological models. WATCH technical report, 22
- Wing IS, De Cian E, Mistry MN (2021) Global vulnerability of crop yields to climate change. *J Environ Econ Manag* 109:102462
- World Bank (2022) World bank development indicators, 2022. data retrieved from World Bank. <https://data.worldbank.org/indicator>
- Zhang P, Zhang J, Chen M (2017) Economic impacts of climate change on agriculture: The importance of additional climatic variables other than temperature and precipitation. *J Environ Econ Manag* 83:8–31
- Zhao C et al (2016) Plausible rice yield losses under future climate warming. *Nature plants* 3(1):1–5
- Zhao C et al (2017) Temperature increase reduces global yields of major crops in four independent estimates. *Proceedings of the national academy of sciences* 114(35):9326–9331